Self-confined light waves in nematic liquid crystals

Highlights

- Review of the nonlinear optics of nematic liquid crystals.
- Reviews the physics and engineering background.
- Reviews the mathematical modelling of the nonlinear optics.
- Includes comparisons between experimental results and mathematical modelling.
- Includes details of the mathematical modelling.

Self-confined light waves in nematic liquid crystals

Gaetano Assanto,
NooEL - Nonlinear Optics & OptoElectronics Lab, University of Rome "Roma Tre",
00146 Rome, Italy
and

Noel F. Smyth
School of Mathematics, University of Edinburgh,
Edinburgh, Scotland, EH9 3FD, U.K.

Abstract

The study of light beams propagating in the nonlinear, dispersive, birefringent and nonlocal medium of nematic liquid crystals has attracted widespread interest in the last twenty years or so. We review hereby the underlying physics, theoretical modelling and numerical approximations for nonlinear beam propagation in planar cells filled with nematic liquid crystals, including bright and dark solitary waves, as well as optical vortices. The pertinent governing equations consist of a nonlinear Schrödinger-type equation for the light beam and an elliptic equation for the medium response. Since the nonlinear and coupled nature of this system presents difficulties in terms of finding exact solutions, we outline the various approaches used to resolve them, pinpointing the good agreement obtained with numerical solutions and experimental results. Measurement and material details complement the theoretical narration to underline the power of the modelling.

1 Introduction

The study of nonlinear dispersive waves originally arose in the context of fluid mechanics, with water waves on the surface of a fluid being a major area of study. The pioneering work by G.G. Stokes, Lord Rayleigh and J. Boussinesq is notable and is analysed, summarised and set in context in the classic book by Lamb [1]. Of note to the present review, in 1834 J. S. Russell observed a new form of water wave, a "wave of translation," now termed solitary wave, on the Union Canal on the western side of Edinburgh, Scotland, U.K., which he later verified with experiments in a wave tank [2]. The new wave was of humped shape, surprising at the time as it was assumed that all waves are essentially Fourier series consisting of oscillatory modes. The reason that such a hump shaped wave can exist is that a solitary wave is a *nonlinear* wave which cannot be predicted on the basis of linear or weakly nonlinear theory [3]. Solitary waves were placed on a sound theoretical basis by Boussinesq in 1871 [4] and Korteweg and de Vries in 1895 [5]. Boussinesq derived a weakly nonlinear, long wave approximation to the water wave equations, the Boussinesq equation, with the (now) famous sech^2 solitary wave profile. Korteweg and de Vries essentially derived a uni-directional form of the Boussinesq equation, now known as the Korteweg-de Vries (KdV) equation [3]. With this sound footing the theoretical study of solitary waves became a backwater, with a dedicated short section in the classic text [1]. This radically changed with the discovery in 1967 that the KdV

equation is exactly integrable in a Hamiltonian sense, with its solution determined by the method of inverse scattering [6]. This prompted an explosion of research into nonlinear dispersive waves, with the resulting discovery that many other such equations are integrable using inverse scattering [3, 7, 8]. These include the nonlinear Schrödinger (NLS) equation, of major interest here, the Sine-Gordon equation and Toda chain, among many others. One consequence of a nonlinear dispersive wave equation being integrable is that N interacting solitary waves of this equation do so "cleanly," with a mere phase shift, but without a change of shape. Due to this particle-like behaviour, the term soliton was coined for the solitary wave solutions of integrable equations. The words soliton and solitary wave are therefore not interchangeable, as a soliton is a specific type of solitary wave, a distinction which is not always observed in the general literature, and even less in experimental reports.

Accompanying this research on nonlinear dispersive waves was its extension into several areas beyond classical water wave theory, including optics, plasma physics and magnetism [3, 8] as well as biology [9]. In addition to these applications to specific areas, new methods to analyse nonlinear dispersive wave equations were developed [3]. One such powerful method is Whitham modulation theory, used to analyse slowly varying modulated waves [3, 10]. It assumes a slowly varying periodic wavetrain and gives a set method to determine modulation equations for its slowly varying parameters, such as amplitude, wavenumber and mean height. Whitham modulation theory not only determines the stability of nonlinear dispersive wavetrains, but is the only known approach to find modulated solutions such as dispersive shock waves, better known as undular bores in fluids [11]. This paper will relate research in and illustrate a particular application of nonlinear wave theory to nonlinear light beams in nematic liquid crystals (NLC) [12, 13, 14]. The key work was the reported evidence that bulk NLC can support stable optical solitary waves— termed nematicons— based on reorientation [15]. As discussed in the next Sections, the equations governing the nonlinear optics of reorientational nematic liquid crystals are $(2+1)$ dimensional and consist of an NLS-type equation for the light beam and an elliptic one for the material response [16]., These equations are not integrable, as witnessed by the fact that nematicons do not interact cleanly [16]. To term nematicons as solitons is therefore not strictly correct, as understood in the applied mathematics literature; in applied physics and optics, however, nematicons are commonly referred to as reorientational (spatial) solitons, nonlocal solitons, self-confined waves in soft matter etc. While it is known that $(2+1)$ dimensional solitary waves governed by NLS-type equations are unstable, exhibiting catastrophic collapse above a power threshold and decaying into diffractive radiation below it [17], this instability does not occur in nematicons as the medium is "nonlocal," in that its response extends far beyond the waist of the beam excitation [16, 18, 19]. The issue of nonlocality will be taken up in detail in Section 3. A major obstacle to the analysis of the pertinent model is that there are no general exact solutions, even in $(1+1)$ dimensions. This lack of exact solitary wave, or periodic wave, solutions implies that standard analytical nonlinear wave techniques, such as Whitham modulation theory, cannot be applied in standard form, let alone inverse scattering. The NLC equations can, of course, be solved numerically, e.g., with pseudo-spectral methods [20, 21] as such techniques are highly suitable for nonlinear dispersive wave equations. Hence, as discussed in Section 4, analytical progress on the nonlinear optics of nematic liquid crystals requires other approximate approaches, including variational methods, an extension of the classical Rayleigh-Ritz approach, as well as extensions of Whitham modulation theory for which a knowledge of exact periodic wave solutions is not needed. As shown in Section 6, surprisingly, but stemming from the highly nonlocality of NLC in many situations, the exact profile of a nematicon is

not necessary in order to analyse its propagation.

It is intuitive that, in the presence of absorption, light beams propagating through NLC can act as energy sources able to heat the medium. This heat is important as the optical properties of NLC, such as refractive indices, elasticity and birefringence, are temperature dependent [22, 23, 24]. Thermo-optic nonlinear changes in NLC can be self-defocusing, while optical reorientation is self-focusing, so that thermal and reorientational effects in response to specific light polarizations can act in opposition. Standard undoped NLC, such as 5CB and E7, are nearly pure dielectric and the thermal contributions are weak; nevertheless these can be enhanced through the addition of dyes [25] or nano-particles [26]. These thermo-optic effects on nematicon behaviour and propagation are addressed in Section 7.

Since their initial report in terms of reorientational self-guided and diffraction-less wave-packets [15], there has been a large amount of experimental investigations of nematicons, their interactions and control, and other nonlinear optical waves, such as optical vortices, in nematic liquid crystals [16]. A great stimulus to the theoretical study of nonlinear optics in NLC has come from these observations and the need to model them. When comparing experimental and theoretical results, NLC are— in some senses— more versatile than fluids such as water and the atmosphere, as the latter are affected by extra effects such as viscosity, turbulence etc. which are not generally accounted for in models. Conversely, light beams in NLC mainly suffer from Rayleigh scattering, leading to decay on millimetre distances, so the results from models and experiments are more prone to good agreement. Section 6 illustrates techniques used to model experiments with light beams in NLC, showing that the approaches mentioned in the previous paragraph yield model equations whose solutions are an excellent match with measurements.

2 Physical background

The physical background and some details on the geometry of nonlinear light beams in planar cells filled with nematic liquid crystals will now be summarised, so that the mathematical analysis and modelling of the succeeding sections can be understood in context. It will be shown that these models, which can be reduced to simpler forms based on the underlying physics, give accurate agreement with experimental results.

Nematic liquid crystals are fluids with a regular crystalline structure encompassing orientational order and positional randomness [12]. The word "nematic" derives from the ancient Greek word *nematos* ($\nu\eta\mu\alpha\tau o\sigma$) meaning thread, as NLC are metaphases consisting of anisotropic (elongated) molecules with their dominant (long) axes oriented along a preferred angular direction. The latter is termed the molecular director and usually indicated by the unit vector $\mathbf{n}$. The valence electrons of these molecules can move more easily along the director, as their backbones are based on benzine rings [13, 14], so that these non-polar NLC molecules are easily polarised in the presence of electric fields. The electronic polarizability of the resulting dipoles and, consequently, the NLC polarization field vector, are usually larger along $\mathbf{n}$ than across it as the benzine rings are linked along the molecular director, yielding refractive indices $n_{\|} > n_{\perp}$ for electric fields parallel and orthogonal to $\mathbf{n}$, respectively, which characterize NLC as positive uniaxial crystals with optic axis corresponding to $\mathbf{n}$ [3, 12]. The two (plane wave) eigensolutions corresponding to a given wavevector $\mathbf{k}$ are ordinary and extra-ordinary waves, with electric field either orthogonal to both $\mathbf{k}$ and $\mathbf{n}$ or co-planar with them, respectively. The extra-ordinary waves in NLC are dispersive and nonlinear through

reorientation [3, 13, 14, 27]. The optical solitary waves addressed in this paper consist of extra-ordinary eigenwaves [28, 29], although ordinary wave beams have been reported to self-focus and confine via a thermo-optic response through light absorption in dye-doped NLC [30, 31, 32, 33], as summarised in Section 7. Wavepackets with mixed eigenstates and polarization evolution owing to birefringence would be subject to geometric phases [34, 35] and compensate diffraction [36, 37, 38], but their self-trapping is not dealt with here.

Let us consider a light beam propagating in NLC with its wavevector $\mathbf{k}$ at an angle θ with respect to $\mathbf{n}$. If the wavepacket is linearly polarised as an extraordinary-wave, e-wave (with the electric field $\mathbf{E}$ coplanar with $\mathbf{n}$ and $\mathbf{k}$), its phase velocity c is θ dependent with

$$c(\theta) = \frac{c_0}{n_e(\theta)} = c_0 \frac{\left[\left(n_\perp^2 - n_\parallel^2\right)\sin^2\theta + n_\parallel^2\right]^{1/2}}{n_\perp n_\parallel}, \tag{1}$$

where c_0 is the speed of light in a vacuum. Its Poynting vector is also θ dependent and forms a walk-off angle δ with respect to the wavevector [3, 39, 40], given by

$$\delta(\theta) = -\frac{1}{n_e(\theta)}\frac{dn_e(\theta)}{d\theta}. \tag{2}$$

At the same time, the dipoles induced by light in the anisotropic molecules react to the electric field $\mathbf{E}$ of the beam, with the resulting electromagnetic torque acting on them. This torque $\mathbf{\Omega}$ is given by

$$\mathbf{\Omega} = \epsilon_0 \Delta\epsilon \left(\mathbf{n}\cdot\mathbf{E}\right)\left(\mathbf{n}\times\mathbf{E}\right), \tag{3}$$

where ϵ_0 is the dielectric susceptibility of the vacuum and $\Delta\epsilon = n_\parallel^2 - n_\perp^2$ the anisotropy at optical frequencies. The torque $\mathbf{\Omega}$, counteracting the elastic intermolecular forces of the nematic medium, acts to reorient the excited dipoles (and therefore the director $\mathbf{n}$) to a larger angle $\theta + \phi$, with ϕ the all-optical (nonlinear) contribution [13, 27]. This response increases the e-wave refractive index n_e, resulting in self-focusing, which eventually supports the formation of graded-index waveguides able to balance beam diffraction and sustain (2+1)D solitary wave-packets, nematicons [16, 41]. Nematicons are spatial optical solitary waves which can be excited by coherent/incoherent light in common NLC mixtures at mW (milli-Watt) power levels by Gaussian or bell-shaped input beams which are a few micrometers wide [16, 28]. For a typical NLC birefringence $n_\parallel - n_\perp \approx 0.2$ (or larger) in the visible or near-infrared at room temperature, the maximum walk-off angle of a beam launched with $\mathbf{k}$ parallel to the down cell direction Z is about 7^o (or larger). This occurs for an orientation $\theta \approx \pi/4$, which also maximizes the nonlinear optical response [18]. As will be shown below, the beam evolution is governed by a nonlinear Schrödinger (NLS) type equation in the slowly varying, paraxial approximation. For NLS-type equations, an input wavepacket will evolve to a steady solitary wave in a non-monotonic, oscillatory fashion, in contrast to the monotonic evolution for Korteweg-de Vries-type equations, with diffractive radiation shed in the process [7]. Owing to beating with this shed radiation, which is trapped by the transverse refractive potential, nematicons breath versus propagation and exhibit power dependent oscillations in peak intensity and transverse size [19]. Under approximations, to be discussed below, this radiation can be assumed to be fully guided, so that the beam never reaches a "true" steady state. In typical samples this radiation is shed on very long propagation scales and the so-called Snyder-Mitchell model [42], which assumes that no diffractive radiation is shed on evolution, retains its validity. Nevertheless, while care must be taken about its long term

predictions due to the neglect of power leakage and losses, in realistic conditions— with finite propagation lengths and proper excitations— nematicons can exhibit a steady appearance with uniform confinement and invariant profile [15].

The generation of nematicons can be mathematically modelled by a partial differential equation (PDE) for the nonlinear reorientational response when extraordinary-wave light beams propagate in the sample, coupled with a PDE governing the response of the perturbed uniaxial dielectric. Physical, dimensional, laboratory coordinates will be denoted by capital letters, (X, Y, Z), while non-dimensional coordinates by lower case letters, (x, y, z). In the next section, the governing equations will be made dimensionless.

The optically induced reorientation angle ϕ is governed by the elliptic equation

$$K\nabla^2\phi + \left[\frac{1}{4}\epsilon_0\Delta\epsilon|A|^2 + \frac{1}{2}\Delta\epsilon_{LF}E_{LF}^2\right]\sin\left(2(\theta+\phi-\delta)\right) = 0, \tag{4}$$

where A is the envelope of the dominant transverse component of the electric field (note that the transverse magnetic field would be more accurate in describing e-wave propagation, see Refs. [43, 44]). E_{LF} is the root mean square amplitude of a low-frequency (LF) electric field applied across the NLC thickness to control its background orientation θ, with $\Delta\epsilon_{LF}$ the LF dielectric anisotropy. Such a contribution describes biased samples with an external voltage to pre-adjust the angle θ to the desired value in order to tune the nonlinearity and avoid a threshold response. The latter stems from the Freedericks transition when $\Omega = 0$ because $\mathbf{n}$ and $\mathbf{E}$ are mutually orthogonal [14, 27], so that a minimum optical power is required to reorientate the nematic molecules, which is undesired as such relatively high powers can lead to medium heating and other unwanted effects. K is a single scalar quantifying the elastic response of the medium. Based on elastic continuum theory, in fact, the spatial distribution of the molecular director undergoes three macroscopic distortions, namely splay, twist and bend, with their energies expressed by

$$\epsilon_{\text{splay}} = \frac{1}{2}K_1(\nabla\cdot\hat{n})^2, \quad \epsilon_{\text{twist}} = \frac{1}{2}K_2(\hat{n}\cdot\nabla\times\hat{n})^2, \quad \epsilon_{\text{bend}} = \frac{1}{2}K_3|\hat{n}\times\nabla\times\hat{n}|^2 \tag{5}$$

respectively, and K_i, $i = 1, 2, 3$, are the pertinent elastic coefficients in the Frank formalism [45]. Choosing a single scalar K for all of these elastic constants greatly simplifies the model without introducing significant error when describing the interaction of a fully ordered nematic phase with electromagnetic eigenwaves.

The beam propagation can— in principle— be described by Maxwell's equations. However, the resulting system of equations is too involved to enable any mathematical modelling, with numerical solutions being the only course [46, 47, 48]. Since most typical experimental conditions can be assumed weakly nonlinear and with a slowly-varying electric field envelope for the beam (that is, with variations over a length scale much longer than the wavelength of the light), a standard multiple scales analysis reduces Maxwell's equations to an NLS-type equation, as is standard for nonlinear, dispersive waves [3, 8, 49]. Hence, in the slowly varying, weakly nonlinear, paraxial approximation the evolution of the beam propagating down the sample along Z in the principal plane defined by the coplanar optic axis $\mathbf{n}$ and wavevector $\mathbf{k}$, containing also the Poynting vector $\mathbf{S}$, the optical field is governed by

$$2ik_0n_e(\theta)\left[\frac{\partial A}{\partial Z} + \tan\delta\frac{\partial A}{\partial T}\right] + \frac{\partial^2 A}{\partial X^2} + \frac{\partial^2 A}{\partial Y^2} + k_0^2\Delta\epsilon\left[\sin^2(\theta+\phi) - \sin^2\theta\right]A = 0, \tag{6}$$

where k_0 is the plane wave propagation constant in vacuum and (T, Z) the principal plane with $T = (X, Y)$. Here, δ, θ and ϕ are angles in (T, Z), and A is the envelope of the electric field

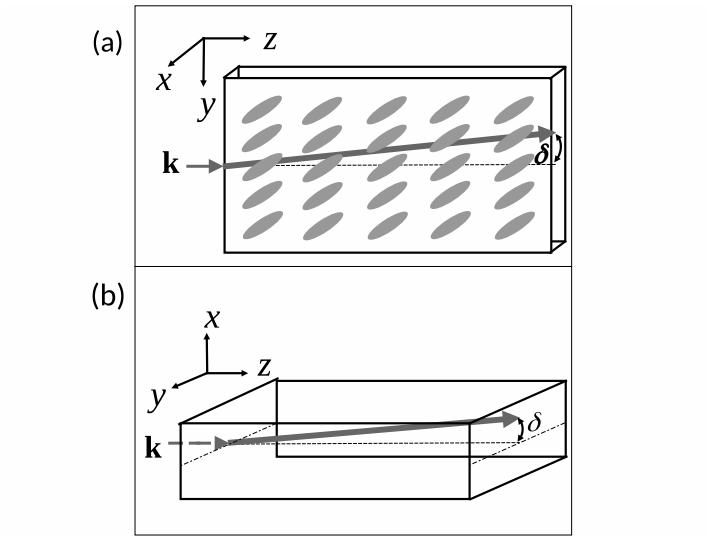

Figure 1: Schematic of typical planar NLC cell configurations showing director orientations. (a) Homogeneous molecular orientation in the width plane (y, z), (b) homogeneous molecular orientation in the thickness plane (x, z). The walk-off angle δ and the wavevector $\mathbf{k}$ of the light beam are shown.

linearly polarized in the same plane. Despite the unavoidable photon scattering stemming from dielectric inhomogeneities (Rayleigh scattering) and the consequent power dissipation, no optical losses have been incorporated in the NLS-type equation (6). The two equations (4) and (6) form a non-dissipative, saturating, nonlinear wave system, inasmuch as the reorientation angle cannot exceed $(0, \pi/2)$. In addition, the nematic liquid crystals' response is nonlocal as the response of the fluid, both elastically and optically, tends to be much wider than the transverse size of the wavepacket. Solitary waves governed by the $(2 + 1)$ dimensional NLS equation are unstable, decaying into radiation below a power threshold and exhibiting catastrophic collapse above it [17]. The nematic system (4) and (6) is a $(2 + 1)$D NLS-type equation free of this instability and catastrophic collapse due to its nonlocal and saturating character [49, 50]. This is witnessed by the director equation (4) being elliptic, so its solution at any point depends on the solution in the whole sample domain, which is the mathematical equivalent of the physical concept of nonlocality. The model (4) and (6) supports stable self-confinement in two transverse dimensions, with robust solitary waves capable of mutual interactions [51, 52]. The latter can be attractive or repulsive depending on the nonlocal range, the separation, the coherence and the relative phase, with a richer phenomenology than their local (Kerr-type) and thermo-optic counterparts [53, 54, 55, 56, 57, 58, 59, 60].

Figure 1 shows a schematic of standard planar cell configurations encompassing (i) homogeneous orientation in the plane (Y, Z) of the sample width or (ii) homogeneous distribution of the molecular director in the plane (X, Z) of the sample thickness. When studying beam evolution in the (Y, Z) plane, geometry (i) allows one to observe walk-off and transverse displacement [61], whereas geometry (ii) permits electro-optical control of the background director orientation θ when applying a voltage via thin film (transparent) electrodes on the cell (upper and lower) interfaces [15]. The latter are chemically treated (e.g., with polyimide) and mechanically rubbed to ensure anchoring of the NLC molecules and therefore uniform

director distribution (angle θ) in the bulk of the sample by means of the elastic forces. The usual separation between the interfaces is of order 100 μm to avoid beam interaction with the boundaries and vignetting effects, but thicknesses as low as 30 μm have been employed as well [62, 63]. Thinner glass interfaces are often mounted at the input and output of the cell in order to seal it and prevent undesired beam depolarization due to the formation of menisci (with unpredictable θ) at the air/NLC boundaries [15, 45].

The optics of and several photonics applications of nematicons have been reviewed over the years [16, 29, 41, 45]. Among the most salient effects and phenomena involving nematicons which have been investigated to date, it is worth underlying that these reorientational spatial solitons are able to guide co-polarised (extra-ordinary wave) signals confined within the multimodal reorientational index well $\Delta n_e = n_e(\theta+\phi) - n_e(\theta)$, regardless of their wavelength [64, 65, 66, 67, 68, 69]. Moreover, since NLC can reorient under external stimuli, such as low-frequency external electric fields, nematicon waveguides can be steered in direction by applying a voltage across the thickness of the cell [61, 70, 71] or in its principal plane [72, 73, 74, 75, 76], such that the background orientation θ is electro-optically modified and, consequently, the inherent walk-off is also. Likewise, external magnetic fields can affect the distribution of the molecular director [77, 78, 79]. Moreover, as the walk-off depends on the overall orientation, $\delta = \delta(\theta + \phi)$, in the highly nonlinear regime with ϕ comparable to θ nematicons can undergo power dependent self-routing [44, 80]. Since the evolution of spatial solitary waves is essentially governed by their main wavevector, nematicons propagating across a graded-index or abrupt dielectric interface are subject to standard or anomalous refraction (depending on the angle of incidence and the orientation of the optic axis) [81, 82, 83], as well as total internal reflection and lateral beam displacement [84, 85]. They also exhibit confinement bistability in cavityless geometries versus beam power [86, 87, 88], applied voltage [89] and angle of incidence [90] and are able to form multicolour, vector and cluster states [55, 91, 92, 93, 94, 95]. Finally, reorientational solitons can coexist/compete with either electronic [65, 96, 97] or thermal responses in NLC [30, 31, 32, 98, 99, 100, 101], yielding novel features in suitably doped materials [67, 102, 103, 104, 105]. The mathematical modelling of the control and manipulation of nematicons will now be discussed below.

3 Nematic Equations

The full, dimensional equations governing the propagation of a light beam in nematic liquid crystals consist of (4) for the NLC response and (6) for the electric field of the beam. As stated in Section 2, the field equation is an NLS-type equation coupled to an elliptic equation for the medium response. The coupling through reorientation is highly nonlinear. Therefore, the system (4) and (6) is difficult to study analytically, with fully numerical approaches the only way to obtain solutions [46, 47, 48]. However, typical light beams used in experiments are of milli-Watt power [16, 28]. For such low powers the optical response ϕ is small compared with the imposed director angle θ, $|\phi| \ll \theta$. In that limit, the system (4) and (6) can be partly linearised by expanding the trigonometric functions in Taylor series to $O(\phi)$. Furthermore, the equations can be simplified by non-dimensionalising the variables. Let us assume that the input wavepacket is a Gaussian beam with power P_0, width $\mathcal{W}$ and electric field of amplitude $\mathcal{E}$, related by

$$P_0 = \frac{\pi}{2}\Gamma\mathcal{E}^2\mathcal{W}^2, \quad \text{with} \quad \Gamma = \frac{1}{2}\epsilon_0 c_0 n_e. \tag{7}$$

For a typical transverse distance W and a typical down cell length D, the non-dimensional space variables (x, y, z) and electric field u can be chosen as

$$Z = Dz, \quad X = Wx, \quad Y = Wy, \quad A = \mathcal{E}u. \tag{8}$$

Non-dimensionalising (4) and (6) we find

$$D = \frac{4n_e}{k_0 \Delta\epsilon \sin 2\theta} \quad \text{and} \quad W = \frac{2}{k_0\sqrt{\Delta\epsilon \sin 2\theta}}, \tag{9}$$

with the non-dimensional governing equations [48, 62, 63, 106, 107]

$$i\frac{\partial u}{\partial z} + i\gamma\Delta\frac{\partial u}{\partial x} + \frac{1}{2}\nabla^2 u + 2\phi u = 0, \tag{10}$$

$$\nu\nabla^2\phi - 2q\phi = -2|u|^2. \tag{11}$$

Here, the Laplacian ∇^2 is in the transverse variables (x, y), the strength of the elastic response is measured by ν and the strength of the low frequency pre-tilting field by q, given by

$$\nu = \frac{4\pi\Gamma K\mathcal{W}^2}{\epsilon_0\Delta\epsilon P_0 W^2 \sin 2\theta}, \quad q = \frac{4\Delta\epsilon_{LF}E_{LF}^2|\cos 2\theta|}{\epsilon_0\Delta\epsilon\mathcal{E}^2 \sin 2\theta}. \tag{12}$$

In addition, the walk-off term in the electric field equation (10), $\Delta = \tan\delta$, gains a scaling factor γ,

$$\gamma = \frac{2n_e}{\sqrt{\Delta\epsilon \sin 2\theta}}. \tag{13}$$

For the typical experimental parameter values cited in Section 2 [16, 28], the nonlocality parameter ν is $O(100)$ [18, 19, 48, 62, 63, 108]. Note that if the walk-off Δ is constant, then it can be factored out via the phase transformation

$$u(x, z) = U(x, z)e^{i\left(\frac{1}{2}\gamma^2\Delta^2 z - \gamma\Delta x\right)}, \tag{14}$$

resulting in

$$i\frac{\partial U}{\partial z} + \frac{1}{2}\nabla^2 U + 2\phi U = 0, \tag{15}$$

$$\nu\nabla^2\phi - 2q\phi = -2|U|^2. \tag{16}$$

While the equations (10) and (11) have been introduced in the context of light beam propagation in nematic liquid crystals, they are much more general. In particular, the same system governs the propagation of light beams in a thermo-optical material for which the refractive index depends on temperature [109, 110, 111, 112]. In this case, the variable ϕ is the medium temperature. The usual system used for thermo-optical media has the parameter $q = 0$, but it can be argued that the structure of the temperature response along z results in a term equivalent to the pre-tilt q in (11) [109, 113]. A system of equations similar to the nematic system also arises in so-called α models of fluid turbulence [114, 115]. Finally, systems of equations resembling the nematic equations (15) and (16) arise in astrophysics. These include the Schrödinger-Newton equations, which arise as a simple model of quantum gravitation [116, 117]. Solitary wave solutions of the Schrödinger-Poisson system, which are the nematic equations with $q = 0$ in the director equation (16), have been used to model

dark matter [118] and the interaction between ordinary and dark matter [119]. The analogy between the nematic equations (in the context of thermo-optic media) has been exploited as analogues of galactic dark matter interactions in order to understand the implications of dark matter models [120]. We argue that the present work, presented through the optics of nematic liquid crystals, then has much broader implications.

The nematic equations (10) and (11), or (15) and (16), can be extended to N incoherently interacting beams [92]

$$i\frac{\partial U_i}{\partial z} + \frac{1}{2}D_i\nabla^2 U_i + 2A_i\phi U_i = 0, \quad i = 1, \dots N, \tag{17}$$

$$\nu\nabla^2\phi - 2q\phi = -2A_i\sum_{i=1}^{N}|U_i|^2. \tag{18}$$

The electric field equations (17) are general, in that the N beams can have different wavelengths, so that the diffraction coefficients D_i and the coupling coefficients A_i can be distinct for each beam. However, for the near-infrared and visible light employed in experiments these coefficients differ by no more than a few percent and so can be taken equal [92, 95].

In their ordered state and with extraordinary waves, nematic liquid crystals are self-focusing, so that the refractive index n_e increases with beam intensity $|u|^2$ and can support bright solitary waves, nematicons. NLC can be used as self-defocusing media when acting on temperature or by the addition of azo dyes [121]. The actual response of the NLC due to absorbing dyes is complicated by the Janossy effect [33, 122], as well as by changes in the order parameters [121]. A simple and convenient approximation in the electric field equation (15), or (10), is a defocussing reorientation, so that

$$i\frac{\partial U}{\partial z} + \frac{1}{2}\nabla^2 U - 2\phi U = 0. \tag{19}$$

It has been shown both experimentally [121] and analytically [123] that azo-doped NLC support dark solitary wave, dark nematicon, solutions.

It is known from numerical solutions that the nematic equations have a solitary wave solution [19], which has been observed experimentally [15, 16, 28]. However, even in its semi-linearised form (10) and (11), there are no known general exact solutions for $\nu \neq 0$. It is noted that in the fully local limit with $\nu = 0$ the equations (15) and (16) reduce to the NLS equation, which in $(1+1)$ dimensions is integrable with known N-soliton solutions. However, in the highly nonlocal case of physical relevance with ν large [18, 19, 62, 63, 108], the only available exact nematicons are isolated solutions for fixed relations between the parameters ν and q and given beam amplitude and width [88, 124]. General solitary waves, conversely, have an arbitrary amplitude which determines the width [3].

In $(1+1)$ dimensions, a nematicon is sought in the form

$$u = f(x)e^{i\sigma z}, \quad \theta = g(x), \tag{20}$$

where f and g are real. Substituting these into the nematic equations (10) and (11) gives that the nematicon is the solution of

$$\frac{d^2 f}{dx^2} + 4gf - 2\sigma f = 0, \quad \frac{d^2 g}{dx^2} + \frac{2}{\nu}f^2 - \frac{2q}{\nu}g = 0. \tag{21}$$

These two ODEs are identical if we set $g = f/\sqrt{2\nu}$ and $\sigma = q/\nu$, resulting in the isolated nematicon solution

$$u = \frac{3q}{2\sqrt{2\nu}} \operatorname{sech}^2\left(\sqrt{\frac{q}{2\nu}}\, x\right) e^{iqz/\nu}, \quad \theta = \frac{3q}{4\nu} \operatorname{sech}^2\left(\sqrt{\frac{q}{2\nu}}\, x\right). \tag{22}$$

The amplitude of this nematicon is fixed by the parameter values. Nevertheless, this isolated solitary wave solution has the sech^2 profile of the KdV soliton, rather than the sech profile of the NLS soliton, which is unexpected as the electric field equation is NLS-type. This exact, isolated solution is not valid in a bias-free sample with $q = 0$ without external pre-tilting. Besides this isolated nematicon, there is a corresponding periodic, cnoidal wave solution expressed in terms of the Jacobi elliptic cosine function cn^2 [125], noting that in the limit of the modulus $m \to 1$, $\operatorname{cn} x \to \operatorname{sech} x$.

A similar isolated nematicon can be found in $(2+1)$ dimensions with

$$u = f(r)e^{i\sigma z} \quad \text{and} \quad \theta = \frac{1}{2\sqrt{2\nu}} f(r) + \frac{\sigma}{2}, \tag{23}$$

where $r^2 = x^2 + y^2$ is the polar distance, on setting $q = 0$, i.e., in a bias-free cell. This solution approaches $\sigma/2$ as $r \to \infty$, so it does not satisfy the linearisation assumption used to derive the system (10) and (11) from the full equations (4) and (6). Again, the director and electric field equations reduce to the single equation

$$\frac{d^2 f}{dr^2} + \frac{1}{r}\frac{df}{dr} + \frac{2}{\sqrt{2\nu}} f^2 = 0. \tag{24}$$

This differential equation is well known in astrophysics as the Lane-Emden equation of the second kind for a cylindrically symmetric self-gravitating fluid of index two governed by Newtonian gravitation [126]. By the transformation

$$f(r) = \frac{\tau \ln r}{r^2} \tag{25}$$

where $\tau' = \rho(\tau)$, it can be converted into Abel's equation [127] for the variable ρ

$$\rho\frac{d\rho}{d\tau} - 4\rho + 4\tau + \frac{2}{\sqrt{2\nu}}\tau^2 = 0. \tag{26}$$

The exact solution of Abel's equation has recently been found [128, 129], but it is very involved and probably of little use for modelling nematicons [88].

There has been some work on the issues of existence, uniqueness and stability of solitary wave solutions of the nematic equations in various forms. These studies do not actually provide any nematicon solutions as such. Hamiltonian methods were used to show the existence and stability of nematicon solutions of the system (10) and (11) in $(2+1)$ dimensions, which are symmetric and decay to zero as $r \to \infty$ [130, 131]. As the proofs were based on energy minimisation, nematicon stability was also proved as a result. In addition, this work gave rigorous mathematical justification of the regularising role of the nonlocal response, but the question of uniqueness was not answered. This theoretical work [131] has important implications for numerical solutions of the nematic equations. It was found that there exists a minimum nematicon power, with the beam decaying into diffractive radiation below this. This result is valid for a continuous system, but numerical solutions of the nematic equations

are based on discrete approximations to the continuous equations. For discrete Hamiltonian systems, there is no power threshold on the existence of a (discrete) nematicon; hence, numerical solutions with low power can be spurious and just a result of discretisation. Mountain pass arguments have also shown existence of ground state and excited nematicon solutions of the system (10) and (11) [132], but without providing these solutions.

To date, there have been no equivalent proofs of existence and stability of nematicon solutions of the full nematic set (4) and (6). However, there exist such results for an extension of the linearised equations (10) and (11) [133]. This work used the equations

$$i\frac{\partial u}{\partial z} + \frac{1}{2}\nabla^2 u + u\sin(2\phi) = 0 \tag{27}$$

for the electric field of the beam and

$$\nu\nabla^2\phi - q\sin(2\phi) = -2|u|^2\cos(2\phi) \tag{28}$$

for the director distribution. This is a saturating extension of the linearised system (10) and (11), obtained from the full set (4) and (6) on non-dimensionalisation, without replacing $\sin\phi$ and $\cos\phi$ by the first terms in their Taylor series. Again, it was found that there exists a stable nematicon above a minimum power threshold, but the question of uniqueness was not addressed. The proof highlighted the role of saturation in stability, giving a mathematical basis for this intuitive concept. The saturating equations (27) and (28) also possess a type of bistable nematicon solution, in that two different director distributions ϕ can support the same nematicon in terms of the electric field u, a "wide" one— much wider than the beam– and a "narrow" one— of width comparable with the beam width— [88]. This is valid even for large values of ν. So the concept of nonlocality— in the sense of a director response much wider than the beam width—, linking this with the magnitude of the elastic parameter ν and the stability of $(2+1)$ dimensional solitary waves, needs to be treated with caution. A proper interpretation is that the director equation, whether linearised as in (11) or saturating as in (28), is elliptic and so its solution at a given point depends on the whole sample domain, as known from basic PDE theory.

4 Approximate Nematicon Solutions

There are no known general solitary wave, or other solutions, of the nematic equations (10) and (11), as discussed in Section 3. Therefore, the use of techniques for approximate solutions has proved popular, the main ones being various forms of variational approaches, essentially the classical Rayleigh-Ritz method. The use of variational methods for approximate solitary wave solutions was pioneered by Anderson [134] and their applications are reviewed in [135]. However, care must be taken with variational approximations and their implications need to be independently verified, say from numerical solutions [88, 136].

Standard applied mathematics techniques for analysing solitary and other waves, including Whitham modulation theory [3], are based on exact solutions of the governing equations whose parameters, such as amplitude and width (wavelength for a periodic wave) are assumed to (slowly) vary. Whitham modulation theory derives so-called modulation equations from a Lagrangian formulation of the governing equation by "averaging" the Lagrangian, that is integrating it over a period (all space for a solitary wave) to eliminate the fast phase dependence in order to retain only the slow space and time variations. The modulation

equations for the wave parameters are then found as variational equations of this averaged Lagrangian. However, as discussed in Section 3, there are no general solitary wave or other solutions of the nematic system (10) and (11). In the absence of exact solutions, "reasonable" approximations or trial functions are used to evaluate averaged Lagrangians [134, 135]. These trial functions can be based on either known solutions of closely related equations or numerical solutions.

Variational methods can then yield accurate approximations to unknown steady solitary and other solutions of nonlinear, dispersive wave equations. They have also been extended to obtain the evolution from initial to steady conditions by adding terms to the trial functions which represent the dispersive or diffractive radiation shed as the beam evolves [137], obtaining excellent agreement with numerical results [136].

The director equation (16) is a linear elliptic equation with a forcing $-2|U|^2$, so that it can, in principle, be solved using a Green function G,

$$\phi = -2\int_{-\infty}^{\infty}\int_{-\infty}^{\infty} G(x-\xi, y-\eta)|U(\xi,\eta)|^2\, d\xi d\eta. \tag{29}$$

The electric field equation (15) then becomes the nonlocal NLS equation

$$i\frac{\partial U}{\partial z} + \frac{1}{2}\nabla^2 U - 4U\int_{-\infty}^{\infty}\int_{-\infty}^{\infty} G(x-\xi, y-\eta)|U(\xi,\eta)|^2\, d\xi d\eta = 0. \tag{30}$$

While this formulation is attractive, it hides difficulties. The Green's function of the director equation (16) is $\exp(-\sqrt{2q/\nu}|x|)$ in $(1+1)$ dimensions and $K_0(\sqrt{\frac{2q}{\nu}}r)$ in $(2+1)$ dimensions, where K_0 is the modified Bessel function of the second kind of order 0. Especially in $(2+1)$ dimensions, it is not realistic to do variational calculations with these Green's functions. Hence, they have been often replaced by a simpler function, usually a Gaussian, with the hope that the resulting predictions based on a simplified kernel are accurate enough. Extreme caution should be exercised though, as predictions with Gaussian functions in the director kernel can be inaccurate when compared with solutions with the actual Green's function [138, 139, 140], so that any solutions obtained using simplified kernels need to be compared with numerical solutions of the actual model. Care must also be taken in the choice of trial function, which should have the correct asymptotic behaviour as $r \to \infty$. This is not so much an issue for bright nematicons as they decay to zero at infinity, but it is for $(1+1)$ dimensional dark nematicons as these approach a constant at infinity, $|u| \to u_0$ as $|x| \to \infty$, with $\phi \to u_0^2/q$ as $|x| \to \infty$ in the director equation (16). Studies of dark nematicons with trial functions without this asymptotic behaviour [141, 142] are questionable. If the trial function is carefully chosen and is close to the actual nematicon (as determined, e.g., from numerical solutions), then its functional form does not greatly affect the variational solution [88, 136, 143, 144], although its accuracy should always be verified against full (numerical) solutions. When these caviats are taken into account, variational methods give solutions in excellent agreement with full numerical solutions of the nematic equations [136, 145, 146, 147].

The literature on variational methods in optics, and nonlinear light beam propagation in nematic liquid crystals in particular [146], is vast and cannot be fully done justice here. The approach— based on choosing a trial function with free parameters, e.g., amplitude and width, substituting it into the Lagrangian before averaging and then obtaining the variational equations for the parameters— will be illustrated below through an application to nematicons.

Besides being useful in overcoming the lack of exact solutions and providing approximations in good agreement with full numerical solutions, variational forms of the nematic equations provide valuable insight into nematicon interactions by making use of mechanical analogies. In the variational approach the equations for the positions and velocities of N interacting nematicons are the same as those for N interacting masses under a Newtonian gravitational potential, with the beam power being the equivalent mass [93, 124, 136, 148, 149, 150, 151]. This is valid independent of the assumed solitary profiles [124]. However, the resulting interaction potential is not the simple inverse separation potential of Newtonian gravitation, but depends nonlinearly on the powers of the individual beams. This analogy has proved beneficial in that standard solutions from Newtonian gravitation were transferred over to NLC optics, for instance the two-body Kepler problem [124, 136, 151] and the three-body Lagrange solution [150], and could be further explored with known gravitation solutions [152].

Let us detail the variational approximation through the gravitational interpretation for two interacting nematicons, the Kepler problem. For simplicity, the diffraction and coupling coefficients in the electric field equations (17) are taken equal and normalised to 1. For $N = 2$, the N beam equations (17) and (18) have the Lagrangian

$$\begin{aligned} L &= i\left(u_1^* u_{1z} - u_1 u_{1z}^*\right) - |\nabla u_1|^2 + 4\phi|u_1|^2 + i\left(u_2^* u_{2z} - u_2 u_{2z}^*\right) - |\nabla u_2|^2 + 4\phi|u_2|^2 \\ &\quad - \nu|\nabla\phi|^2 - 2q\phi^2. \end{aligned} \tag{31}$$

Let us keep the trial functions for the beams and the director response general and set

$$\begin{aligned} u_1 &= a_{u_1} f_{u_1}\left(\frac{\zeta_{u_1}}{w_{u_1}}\right) e^{i\sigma_{u_1} + iU_{u_1}(x-\xi_{u_1}) + iV_{u_1}(y-\eta_{u_1})}, \\ u_2 &= a_{u_2} f_{u_2}\left(\frac{\zeta_{u_2}}{w_{u_2}}\right) e^{i\sigma_{u_2} + iU_{u_2}(x-\xi_{u_2}) + iV_{u_2}(y-\eta_{u_2})}, \\ \phi &= \alpha_{u_1} g_{u_1}\left(\frac{\zeta_{u_1}}{\beta_{u_1}}\right) + \alpha_{u_2} g_{u_2}\left(\frac{\zeta_{u_2}}{\beta_{u_2}}\right), \end{aligned} \tag{32}$$

where the profiles f_{u_1} and f_{u_2} and the responses g_{u_1} and g_{u_2} are not specified. Here,

$$\zeta_{u_1} = \sqrt{(x-\xi_{u_1})^2 + (y-\eta_{u_1})^2}, \quad \zeta_{u_2} = \sqrt{(x-\xi_{u_2})^2 + (y-\eta_{u_2})^2}. \tag{33}$$

The positions and velocities of the beams are (ξ_{u_1}, η_{u_1}), (U_{u_1}, V_{u_1}) and (ξ_{u_2}, η_{u_2}), (U_{u_2}, V_{u_2}), respectively. At this point, the functions (32) are substituted into the Lagrangian (31), which is averaged by integrating in x and y from $-\infty$ to ∞ [3] to yield the averaged Lagrangian $\mathcal{L}$. Taking variations of $\mathcal{L}$ with respect to the beam and director parameters gives the modulation equations governing the interaction. Unfortunately, the cross integrals involving u_1 and u_2 cannot be evaluated without assuming their functional forms. Hence, we assume the beams to be Gaussian

$$f_u(r) = f_v(r) = e^{-r^2}, \tag{34}$$

and the cross integrals become

$$\begin{aligned} \int_{-\infty}^{\infty}\int_{-\infty}^{\infty} \phi|u_1|^2\, dxdy &= \alpha_{u_1} a_{u_1}^2 w_{u_1}^2 I_{12u_1} + \frac{\alpha_{u_2} a_{u_1}^2 \beta_{u_2}^2 w_{u_1}^2}{2(w_{u_1}^2 + 2\beta_{u_2}^2)} e^{-\rho^2/(w_{u_1}^2 + 2\beta_{u_2}^2)} \\ \int_{-\infty}^{\infty}\int_{-\infty}^{\infty} \phi|u_2|^2\, dxdy &= \alpha_{u_2} a_{u_2}^2 w_{u_2}^2 I_{12u_2} + \frac{\alpha_{u_1} a_{u_2}^2 \beta_{u_1}^2 w_{u_2}^2}{2(w_{u_2}^2 + 2\beta_{u_1}^2)} e^{-\rho^2/(w_{u_2}^2 + 2\beta_{u_1}^2)} \end{aligned}$$

$$\begin{aligned}
\int_{-\infty}^{\infty}\int_{-\infty}^{\infty} |\nabla\phi|^2\, dxdy &= I_{dpu_1}\alpha_{u_1}^2 + I_{dpu_2}\alpha_{u_2}^2 + \frac{2\alpha_{u_1}\alpha_{u_2}\beta_{u_1}^3\beta_{u_2}^3}{\left(\beta_{u_1}^2+\beta_{u_2}^2\right)^2}\left[1-\frac{\rho^2}{\beta_{u_1}^2+\beta_{u_2}^2}\right]e^{-\rho^2/(\beta_{u_1}^2+\beta_{u_2}^2)} \\
\int_{-\infty}^{\infty}\int_{-\infty}^{\infty} \phi^2\, dxdy &= I_{du_12}\alpha_{u_1}^2\beta_{u_1}^2 + I_{d2u_2}\alpha_{u_2}^2\beta_{u_2}^2 + \frac{\alpha_{u_1}\alpha_{u_2}\beta_{u_1}^2\beta_{u_2}^2}{\beta_{u_1}^2+\beta_{u_2}^2}e^{-\rho^2/(\beta_{u_1}^2+\beta_{u_2}^2)}. \qquad (35)
\end{aligned}$$

Here, the beam separation ρ is

$$\rho^2 = \left(\xi_{u_1}-\xi_{u_2}\right)^2 + \left(\eta_{u_1}-\eta_{u_2}\right)^2. \qquad (36)$$

The integrals arising in the averaged Lagrangian and involving self-interactions are

$$\begin{aligned}
I_{2u_1} &= \int_0^\infty r f_{u_1}^2(r)\, dr, & I_{2u_2} &= \int_0^\infty r f_{u_2}^2(r)\, dr, \\
I_{2pu_1} &= \int_0^\infty r\left(\frac{df_{u_1}(r)}{dr}\right)^2 dr, & I_{2pu_2} &= \int_0^\infty r\left(\frac{df_{u_2}(r)}{dr}\right)^2 dr, \\
I_{12u_1} &= \int_0^\infty r g_{u_1}\left(\frac{w_{u_1}}{\beta_{u_1}}r\right) f_{u_1}^2(r)\, dr, & I_{12u_2} &= \int_0^\infty r g_{u_2}\left(\frac{w_{u_2}}{\beta_{u_2}}r\right) f_{u_2}^2(r)\, dr, \\
I_{dpu_1} &= \int_0^\infty r\left(\frac{dg_{u_1}(r)}{dr}\right)^2 dr, & I_{dpu_2} &= \int_0^\infty r\left(\frac{dg_{u_2}(r)}{dr}\right)^2 dr, \\
I_{du_12} &= \int_0^\infty r g_{u_1}^2(r)\, dr, & I_{du_22} &= \int_0^\infty r g_{u_2}^2(r)\, dr. \qquad (37)
\end{aligned}$$

The actual values of these integrals cancel out when the variational equations for the positions and velocities are calculated, and so their values are not needed. The averaged Lagrangian is

$$\mathcal{L} = \mathcal{T} - \mathcal{P}, \qquad (38)$$

with the kinetic energy $\mathcal{T}$ and potential energy $\mathcal{P}$ expressed as

$$\begin{aligned}
\mathcal{T} &= -2I_{2u_1}a_{u_1}^2w_{u_1}^2\left(\sigma_{u_1}' - U_{u_1}\xi_{u_1}' - V_{u_1}\eta_{u_1}'\right) - I_{2pu_1}a_{u_1}^2 - I_{2u_1}a_{u_1}^2w_{u_1}^2\left(U_{u_1}^2+V_{u_1}^2\right) \\
&\quad + 4I_{12u_1}\alpha_{u_1}a_{u_1}^2w_{u_1}^2 - 2I_{2u_2}a_{u_2}^2w_{u_2}^2\left(\sigma_{u_2}' - U_{u_2}\xi_{u_1}' - V_{u_2}\eta_{u_2}'\right) - I_{2pu_2}a_{u_2}^2 \\
&\quad - I_{2u_2}a_{u_2}^2w_{u_2}^2\left(U_{u_2}^2+V_{u_2}^2\right) + 4I_{12u_2}\alpha_{u_2}a_{u_2}^2w_{u_2}^2 - \nu I_{dpu_1}\alpha_{u_1}^2 - \nu I_{dpu_2}\alpha_{u_2}^2 \\
&\quad - 2qI_{du_12}\alpha_{u_1}^2\beta_{u_1}^2 - 2qI_{du_22}\alpha_{u_2}^2\beta_{u_2}^2 \qquad (39)
\end{aligned}$$

and

$$\begin{aligned}
\mathcal{P} &= \frac{2\nu\alpha_{u_1}\alpha_{u_2}\beta_{u_1}^2\beta_{u_2}^2}{\left(\beta_{u_1}^2+\beta_{u_2}^2\right)^2}\left[1-\frac{\rho^2}{\beta_{u_1}^2+\beta_{u_2}^2}\right]e^{-\rho^2/(\beta_{u_1}^2+\beta_{u_2}^2)} + \frac{2q\alpha_{u_1}\alpha_{u_2}\beta_{u_1}^2\beta_{u_2}^2}{\beta_{u_1}^2+\beta_{u_2}^2}e^{-\rho^2/(\beta_{u_1}^2+\beta_{u_2}^2)} \\
&\quad - \frac{2\alpha_{u_2}a_{u_1}^2w_{u_1}^2\beta_{u_2}^2}{w_{u_1}^2+2\beta_{u_2}^2}e^{-\rho^2/(w_{u_1}^2+2\beta_{u_2}^2)} - \frac{2\alpha_{u_1}a_{u_2}^2w_{u_2}^2\beta_{u_1}^2}{w_{u_2}^2+2\beta_{u_1}^2}e^{-\rho^2/(w_{u_2}^2+2\beta_{u_1}^2)}. \qquad (40)
\end{aligned}$$

It is apparent that the potential of the nematicon interaction is much more complicated than the inverse separation potential of Newtonian gravitation, as it depends in a detailed fashion on the beam and director response parameters.

The modulation equations for the interacting beams can be made to resemble the Kepler two-body problem equations after defining the vector positions $\vec{\xi}_{u_1} = (\xi_{u_1}, \eta_{u_1})$, $\vec{\xi}_{u_2} = (\xi_{u_2}, \eta_{u_2})$,

and the vector velocities $\vec{V}_{u_1} = (U_{u_1}, V_{u_1})$, $\vec{V}_{u_2} = (U_{u_2}, V_{u_2})$. We also define the relative beam separation $\vec{\rho}$ by

$$\vec{\rho} = \vec{\xi}_{u_1} - \vec{\xi}_{u_2}, \tag{41}$$

and the "masses" M_{u_1} and M_{u_2} (beam powers) by

$$M_{u_1} = 2I_{2u_1} a_{u_1}^2 w_{u_1}^2, \quad M_{u_2} = 2I_{2u_2} a_{u_2}^2 w_{u_2}^2. \tag{42}$$

Before taking variations of the averaged Lagrangian (38) with respect to the beam positions and velocities and so obtain equations for their trajectories, the role of the large nonlocality ν needs to be factored in. In the presence of a highly nonlocal response, the beams shed a small amount of diffractive radiation on a long z scale of $O(\sqrt{\nu})$ [145]. Their rate of power decay is then limited, so that as a first approximation the powers M_{u_1} and M_{u_2} of the individual beams are conserved [144]. With this assumption the modulation equations (after taking variations of the averaged Lagrangian (31) with respect to ξ_{u_1}, ξ_{u_2}, η_{u_1}, η_{u_2}, U_{u_1}, U_{u_2}, V_{u_1} and V_{u_2}) are

$$\frac{d}{dz} M_{u_1} \vec{V}_{u_1} = -\left(\frac{\partial \mathcal{P}}{\partial \xi_{u_1}}, \frac{\partial \mathcal{P}}{\partial \eta_{u_1}} \right), \quad \frac{d}{dz} M_{u_2} \vec{V}_{u_2} = -\left(\frac{\partial \mathcal{P}}{\partial \xi_{u_2}}, \frac{\partial \mathcal{P}}{\partial \eta_{u_2}} \right), \tag{43}$$

and

$$\frac{d\vec{\xi}_{u_1}}{dz} = \vec{V}_{u_1}, \quad \frac{d\vec{\xi}_{u_2}}{dz} = \vec{V}_{u_2}. \tag{44}$$

The position equations (43) are Newton's Second Law for the momenta $M_{u_1}\vec{V}_{u_1}$ and $M_{u_2}\vec{V}_{u_2}$. The two nematicons' "centre of mass" can be defined as

$$\vec{R} = \frac{M_{u_1}\vec{\xi}_{u_1} + M_{u_2}\vec{\xi}_{u_2}}{M_{u_1} + M_{u_2}}. \tag{45}$$

In this centre-of-mass system, the distance from the origin ρ is given in (36) and the polar angle is ψ. The system of the two nematicons conserves the angular momentum L_m, with

$$L_m = \rho^2 \frac{d\psi}{dz}. \tag{46}$$

In the centre-of-mass coordinates the mechanical equations (43) and (44) become

$$\frac{d^2\vec{R}}{dz^2} = \vec{0} \quad \text{and} \quad \frac{d^2\rho}{dz^2} - L_m^2 \rho^{-3} = -\frac{M_{u_1} + M_{u_2}}{M_{u_1} M_{u_2}} \frac{\partial \mathcal{P}}{\partial \rho}. \tag{47}$$

This final system for the beam trajectories is the same as for the Kepler two-body problem [153]. These modulation equations give solutions in excellent agreement with the vector nematicon system (15) and (18) [124, 136, 150]; as expected by the conserved power approximation, the disagreement with numerical solutions as z grows due to the effect of the shed diffractive radiation. In addition, beam u_1 generates a so-called shadow beam in u_2 at its position, and vice-versa [124], which is not accounted for in the trial functions (32). These shadow beams can be seen in Figure 2.

As discussed, diffractive radiation can impact on nematicon evolution. Its calculation and inclusion for evolving solitary waves is, in general, non-trivial. A general method, using the perturbed inverse scattering solution of the integrable NLS equation [137], yielded that the

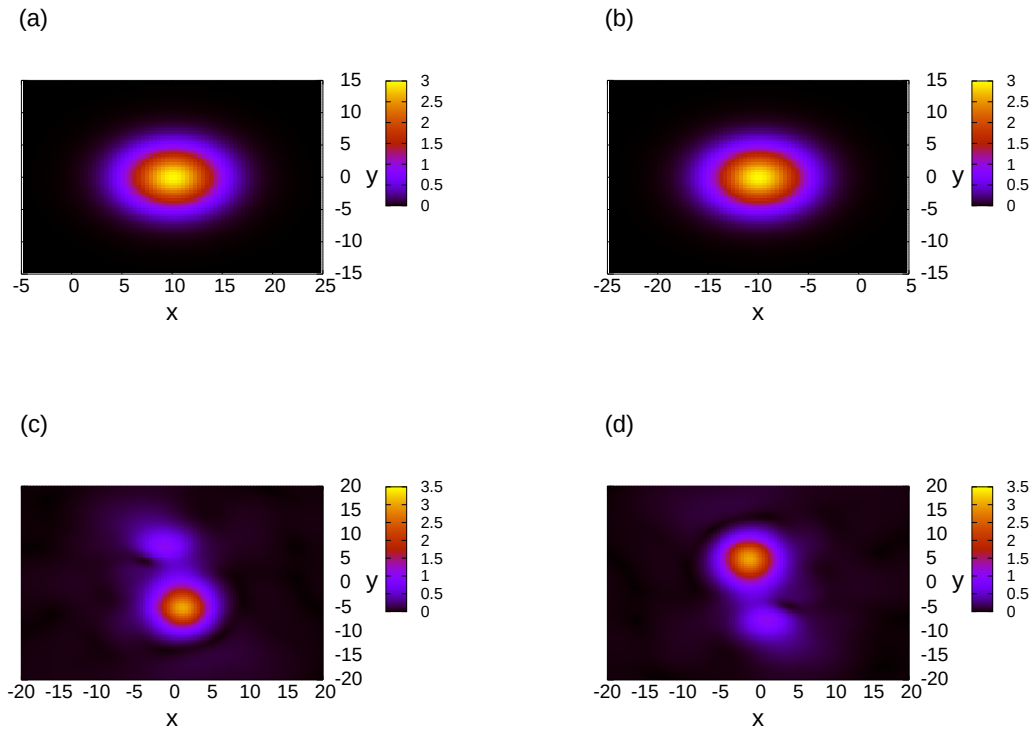

Figure 2: Numerical solutions of system (17)–(18). (a) $|u_1|$ at $z = 0$; (b) $|u_2|$ at $z = 0$; (c) $|u_1|$ at $z = 300$; (d) $|u_2|$ at $z = 300$. The initial beam parameters are $a_{u_1} = a_{u_2} = 3.0$, $w_{u_1} = w_{u_2} = 4.5$, $\xi_{u_1} = 10.0$, $\xi_{u_2} = -10.0$, $\eta_{u_1} = \eta_{u_2} = 0$, $U_{u_1} = V_{u_1} = 0.05$, $U_{u_2} = V_{u_2} = -0.05$. The NLC parameters are $\nu = 500$ and $q = 2$. Figure reproduced from [124].

form of the shed radiation can be deduced without full reliance on inverse scattering and applies to general nonlinear, dispersive wave equations of NLS-type. It was later used to incorporate the effect of this radiation on nematicons [145]. The nematic equations (17) and (18) have the Lagrangian

$$L = i\,(U^*U_z - UU_z^*) - |\nabla U|^2 + 4\phi|U|^2 - \nu|\nabla\phi|^2 - 2q\phi^2. \tag{48}$$

Coming to the choice of suitable trial functions, for a nematicon either a Gaussian or the sech NLS soliton yields good agreement with numerical solutions [88, 136]. We shall use the sech profile

$$U = \left(a\,\mathrm{sech}\,\frac{r}{w} + ig\right)e^{i\sigma}, \quad \phi = \alpha\,\mathrm{sech}^2\,\frac{r}{\beta}, \tag{49}$$

where $r^2 = x^2 + y^2$ and the parameters a, w, g, σ, α and β depend on z. The trial function for the electric field includes the shelf term ig, which comes from the cited NLS study [137]. Inverse scattering shows that the radiation component of a perturbed solitary wave, the continuous spectrum, is of low wavenumber in the vicinity of the evolving soliton [137]. From wave kinematics, in fact, since the dispersion relation for linear, dispersive waves of the nematic equations is $\omega = -|\mathbf{k}|^2/2$, their group velocity is $\mathbf{c}_g = -\mathbf{k}$. Hence, low wavenumber waves have low group velocity and accumulate in the proximity of the propagating nematicon,

consistent with perturbed inverse scattering for the NLS equation. It is worth pin-pointing, from the trial function for the electric field, that the shelf and the nematicon are $\pi/2$ out of phase, as inverse scattering shows that the in-phase component corresponds to changes in the beam width, encompassed in w in the trial function. This radiation can be observed in Figure 3, displaying a numerical solution of the nematic equations (17) and (18): the shelf is the extended region of amplitude around 1 encircling the nematicon. This radiation takes conserved quantities away from the propagating solitary wave so that it can evolve to a steady state. Because of its limited extent, g can be taken non-zero in $0 \leq r \leq \ell$ and the shed light can then be calculated from a linearised equation as it has low amplitude [137]. We shall illustrate these concepts using the nematic equations (17) and (18).

Substituting the trial (49) into the Lagrangian (48) and averaging by integrating in x and y from $-\infty$ to ∞ gives the averaged Lagrangian [145]

$$\begin{aligned}\mathcal{L} &= -2\left(a^2w^2I_2+\Lambda g^2\right)\sigma' - 2I_1aw^2g' + 2I_1gw^2a' + 4I_1awgw' - a^2I_{22} - 4\nu I_{42}\alpha^2 \\ &\quad - 2qI_4\alpha^2\beta^2 + \frac{2A^2B^2\alpha a^2\beta^2w^2}{A^2\beta^2+B^2w^2}. \end{aligned} \tag{50}$$

Here, Λ is the area of the radiation shelf, modulo 2π,

$$\Lambda = \frac{1}{2}\ell^2. \tag{51}$$

The integrals I_1, I_2, I_4, I_{42} and I_{22} in $\mathcal{L}$ are

$$\begin{aligned} I_1 &= \int_0^\infty x\,\mathrm{sech}\,x\,dx = 2C, & I_2 &= \int_0^\infty x\,\mathrm{sech}^2\,x\,dx = \ln 2, \\ I_{22} &= \int_0^\infty x\,\mathrm{sech}^2\,x\tanh^2 x\,dx = \frac{1}{3}\ln 2 + \frac{1}{6}, & I_4 &= \int_0^\infty x\,\mathrm{sech}^4\,x\,dx = \frac{2}{3}\ln 2 - \frac{1}{6}, \\ I_{42} &= \int_0^\infty x\,\mathrm{sech}^4\,x\tanh^2 x\,dx = \frac{2}{15}\ln 2 + \frac{1}{60}, & I_{x32} &= \int_0^\infty x^3\,\mathrm{sech}^2\,x\,dx = 1.352301002\ldots. \end{aligned} \tag{52}$$

where C is the Catalan constant $C = 0.915965594\ldots$ [154] and

$$A = \frac{2I_2}{\sqrt{I_{x32}}}, \qquad B = \sqrt{2I_2}. \tag{53}$$

Taking variations of $\mathcal{L}$ with respect to the beam and director parameters yields the modulation equations

$$\frac{d}{dz}\left(I_2a^2w^2+\Lambda g^2\right) = 0, \tag{54}$$

$$\frac{d}{dz}\left(I_1aw^2\right) = \Lambda g\frac{d\sigma}{dz}, \tag{55}$$

$$I_1\frac{dg}{dz} = \frac{I_{22}a}{2w^2} - \frac{A^2B^4\alpha aw^2\beta^2}{\left(A^2\beta^2+B^2w^2\right)^2}, \tag{56}$$

$$I_2\frac{d\sigma}{dz} = -\frac{I_{22}}{w^2} + \frac{A^2B^2\alpha\beta^2\left(A^2\beta^2+2B^2w^2\right)}{\left(A^2\beta^2+B^2w^2\right)^2}, \tag{57}$$

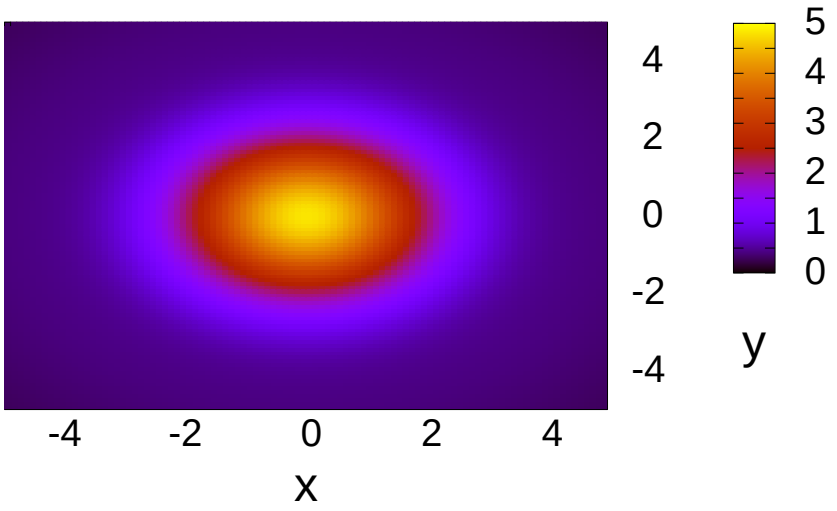

Figure 3: Numerical solution of nematic equations (17) and (18) for $|u|$ at $z = 10$ for the initial condition (49) with $a = 2$, $w = 3.5$ and $g = 0$. The NLC parameters are $\nu = 200$ and $q = 2$.

plus the algebraic equations

$$\alpha = \frac{A^2B^2\beta^2w^2a^2}{2\left(A^2\beta^2 + B^2w^2\right)\left(2\nu I_{42} + qI_4\beta^2\right)} \quad \text{and} \quad \alpha = \frac{A^2B^4w^4a^2}{qI_4\left(A^2\beta^2 + B^2w^2\right)^2}. \tag{58}$$

The parameters α and β are determined by algebraic equations as the director equation (18) does not have z derivatives. These modulation equations do not yet include the role of the diffractive radiation shed as the beam evolves.

The inclusion of radiation loss is more difficult than for the ($(1 + 1)$ dimensional) NLS equations as the nematic equations are $(2 + 1)$ dimensional. As the shed radiation has small amplitude relative to the nematicon, it can be determined from the linearised electric field equation (17)

$$i\frac{\partial U}{\partial z} + \frac{1}{2}\frac{\partial^2 U}{\partial r^2} + \frac{1}{2r}\frac{\partial U}{\partial r} = 0, \tag{59}$$

which can be solved using Laplace transforms [155]. The key quantity needed is the "mass" (optical power) transferred into radiation. The linearised electric field equation (59) has the mass (power) conservation equation

$$i\frac{\partial}{\partial z}\left(r|U|^2\right) + \frac{1}{2}\frac{\partial}{\partial r}\left(rU^*U_r - rUU_r^*\right) = 0. \tag{60}$$

If we assume that the diffractive radiation starts at the edge of the shelf at $r = \ell$, then integrating over it gives the flux to/from the evolving nematicon as

$$\frac{d}{dz}\int_\ell^\infty r|U|^2\,dr = Im\left(rU^*U_r\right)|_{r=\ell} + O(\dot{\ell}(z)). \tag{61}$$

It is then apparent that we need a relation between U_r and U at the shelf edge. Solving the radiation equation (59) by means of Laplace transforms gives

$$U_r|_{r=\ell} = -\frac{1}{2\pi i}\int_C \sqrt{2s}\,e^{-i\pi/4}\frac{K_1\left(\sqrt{2s}\,e^{-i\pi/4}\ell\right)}{K_0\left(\sqrt{2s}\,e^{-i\pi/4}\ell\right)}\,\bar{U}(\ell,s)e^{sz}\,ds, \tag{62}$$

where s is the transform variable and C is the standard Laplace-transform inversion contour, with K_0 and K_1 the modified Bessel functions of the second kind of order 0 and 1, respectively. While this contour integral formally determines the mass flux from the nematicon into shed radiation, it is too involved to be of much use. To obtain a manageable result, the integral (62) can be evaluated in the limit $z \to \infty$ using the method of steepest descent [155], providing the asymptotic result

$$U_r = -\frac{\sqrt{2\pi}}{4e\ell}\int_0^z \frac{R(z')}{z-z'}\frac{1}{\left[(1/2)\log((z-z')/\Lambda) - i\pi/4\right]^2 + \pi^2/4}\,dz' \tag{63}$$

as $z \to \infty$. Here,

$$R^2 = \frac{1}{\tilde{\Lambda}}\left[I_2a^2w^2 - I_2\hat{a}^2\hat{w}^2 + \tilde{\Lambda}g^2\right], \quad \tilde{\Lambda} = \frac{1}{2}\left[7\beta\,\mathrm{sech}^{-1}(1/\sqrt{2})\right]^2. \tag{64}$$

is the difference between the mass of the nematicon plus shelf and the mass of the steady nematicon $2\hat{a}^2\hat{w}$, where $\hat{}$ denotes steady state. As the energy

$$I_{22}a^2 + 4\nu I_{42}\alpha^2 + 2qI_4\alpha^2\beta^2 - \frac{2A^2B^2\alpha a^2w^2\beta^2}{A^2\beta^2 + B^2w^2} = \text{constant} \tag{65}$$

is conserved for the nematic equations, these steady state values can be determined from the initial condition and this conservation law [145]. This excess mass in the beam drives its evolution as it needs to be shed to reach a steady state. After some manipulation, this radiation can be incorporated into the modulation equations (54)–(58) by adding loss to the modulation equation (56) [137, 145], so that it becomes

$$I_1\frac{dg}{dz} = \frac{I_{22}a}{2w^2} - \frac{A^2B^4\alpha a w^2\beta^2}{\left(A^2\beta^2 + B^2w^2\right)^2} - 2\varsigma g, \tag{66}$$

where the coefficient ς derived from the loss (63) with the radiation flux equation (61) is

$$\varsigma = -\frac{\sqrt{2\pi}I_1}{32eR\tilde{\Lambda}}\int_0^z \frac{\pi R(z')\ln((z-z')/\tilde{\Lambda})}{\left\{[\frac{1}{4}\log((z-z')/\tilde{\Lambda})]^2 + 3\pi^2/16\right\}^2 + \pi^2\left[\log((z-z')/\tilde{\Lambda})\right]^2/16}\,\frac{dz'}{(z-z')} \tag{67}$$

It is convenient to drop the mass modulation equation (42) and replace it by the energy equation (65), as the latter is required for the determination of radiation loss. The resulting modulation equations with loss provide solutions in excellent agreement with numerical solutions of the nematic equations [145].

A special case of the modulation equations is the steady state $g = 0$ and $a' = w' = 0$. This gives the variational approximation to the nematicon solution with the amplitude/width relation

$$I_{22} = \frac{2A^2B^4\alpha w^4\beta^2}{\left(A^2\beta^2 + B^2w^2\right)^2} \tag{68}$$

and phase

$$\sigma = \frac{A^4B^2\alpha\beta^4}{\left(A^2\beta^2 + B^2w^2\right)^2}\, z. \tag{69}$$

This approximate nematicon solution agrees well with full numerical solutions of the nematic equations [88].

Standard perturbed solitary wave theory and variational approximations treat the solitary waves as particles as they are averaged out in determining the modulation equations [156]. This approximation can be improved to treat the solitary wave as an extended entity, using methods similar to those for calculating Newtonian gravitational fields due to non-point masses [157]. The extended character of nonlocal solitary waves is important and this extension yields marked improvements when studying nematicons and their trajectories, as they can interact through their tails [143, 144], which is not fully included in particle approximations.

The ability of variational methods to be accurate when compared with numerical solutions and experimental results has prompted widespread analyses of the propagation and interaction of both solitary waves and optical vortices (which will be detailed further in Section 5), as well as their control, in nematic liquid crystals [136]. The modelling of experiments in NLC will be dealt with in Section 6. Some examples include describing the refraction and total internal reflection of nematicons and vortices at interfaces [158, 159, 160, 161, 162], the former in notable agreement with experiments carried out across graded interfaces defined by using planar electrodes and external electric fields to differently orient two adjacent NLC regions [163]. Refraction and reflection of nematicons were also achieved/measured using discrete or interdigitated electrodes [76, 164], or acting with external light beams on the anchoring at the cell boundaries [165]. In many respects, the refraction and total internal reflection of nematicons across a dielectric interface resemble those of linear plane waves. However, the medium birefringence and the extended profile of nematicons do play a role. For instance, nematicons can undergo a lateral shift upon total internal reflection when travelling from a denser to a rarer NLC region [166], with their centre passing through the dielectric boundary twice and the whole beam refracting back into the incident side. As the nematicon equivalent mass relates to power, the shift upon reflection is mass dependent and refraction— called anomalous when wavevector and walk-off angles compete in such a way that the beam appears to emerge from the same half-plane of origin— can change from positive to anomalous versus input power, owing to reorientation [82, 83, 84, 167]. The refraction of nematicons through dielectric interfaces can be extended to trajectory control via localised changes in NLC refractive index, which act as lenses for the beam [168, 169]. If the nematicon is much narrower than the refractive index perturbation, then the nematicon remains stable upon refraction. However, if the nematicon width and the perturbation have comparable sizes, then the former can be de-stabilised [169]. The refraction and total internal reflection of optical vortices across dielectric interfaces show similar properties as nematicons, with one major exception [161, 162] occurring when the refractive index change is above a threshold contrast, such that the NLC perturbation triggers the standard mode-2 azimuthal vortex instability [170], causing the vortex to break up into nematicons.

For simplicity, when using variational approximations it is often assumed that the light beam is far enough from the cell boundaries so that their influence can be ignored. This is valid, e.g., if there is a pre-tilting field so that $q \neq 0$, a voltage-biased cell, so that both the director and electromagnetic (optical) field distributions decay exponentially away from the beam axis [131]. However, nematicon interplays with boundaries were analysed [171, 172, 173, 174, 175] to reveal that boundaries repel the beams. Since this interaction is mass (power) dependent [176], nonlinear repulsion in finite cells was exploited for the experimental demonstration of nematicon trajectory control [177].

Another intriguing possibility offered by NLC is all-optical control via the interaction of one or multiple nematicons and/or external magnetic and electric fields, including the capacitive effects of light valves in voltage-biased cells with a photoconductive interface [70]. In these planar geometries, orthogonally propagating control beams can alter the refractive index and act on the mutual interaction of nematicons, allowing for all-optical switching layouts [71, 178, 179]. Light-by-light control can also be exploited to nonlinearly modify the local refractive index and the beam path [180, 181].

As previously discussed in the context of mechanical analogies for interacting nematicons and Newtonian gravitation, beam-on-beam interactions can control individual trajectories [55, 91, 92, 93, 143, 144, 182, 183]. They have also been studied using variational and Gaussian approximations to the actual response G in the nonlocal NLC equation (30) [184, 185]. A further use of the interaction of nematicons is the generation of higher order (excited state) solitary waves with nodes [186]. These higher order solitary waves were experimentally generated as vector modes consisting of the fundamental nematicon and the excited state.

5 Optical Vortices

Besides bright nematicons, nematic liquid crystals can also support optical vortices, doughnut shaped beams resembling vortices in fluids. In optical vortices the wavefront is twisted in the direction of propagation to have a corkscrew form, resulting in a circulating azimuthal phase and a phase singularity with an amplitude/intensity node at their centres. Optical vortices have wide ranging applications, including the trapping and manipulation of small particles in biology, physics and other areas [187], microscopy [188], astronomy [189, 190, 191, 192] and communications [193, 194]. A number of different components can be used to experimentally generate their phase structure, including spiral phase plates, diffractive elements and computer-generated holograms, segmented deformable mirrors and nanostructured glass plates. In nematic liquid crystals, optical vortices have been generated and manipulated in light-valve geometries, as well as droplets [195, 196, 197, 198, 199].

In media with a local response, optical vortices are unstable to a mode-2 azimuthal instability, so that the vortex breaks up into two beams [17, 200]. This can be seen on solving the nematic equations (15) and (16) in the local limit with the vortex-type initial condition

$$u = are^{-\frac{r^2}{w^2}+i\varphi}, \tag{70}$$

where (r, φ) are plane polar coordinates. Figures 4(a) and (b) show the evolution of this vortex beam for $\nu = 0.5$, which corresponds to the NLC local response. This mode-2 beam break-up can be clearly seen. However, optical vortices are stable in media whose response is nonlocal enough, which can be seen from Figures 4(c) and (d) which present the evolution of the vortex initial condition (70) for the large nonlocality $\nu = 200$. The initial vortex has

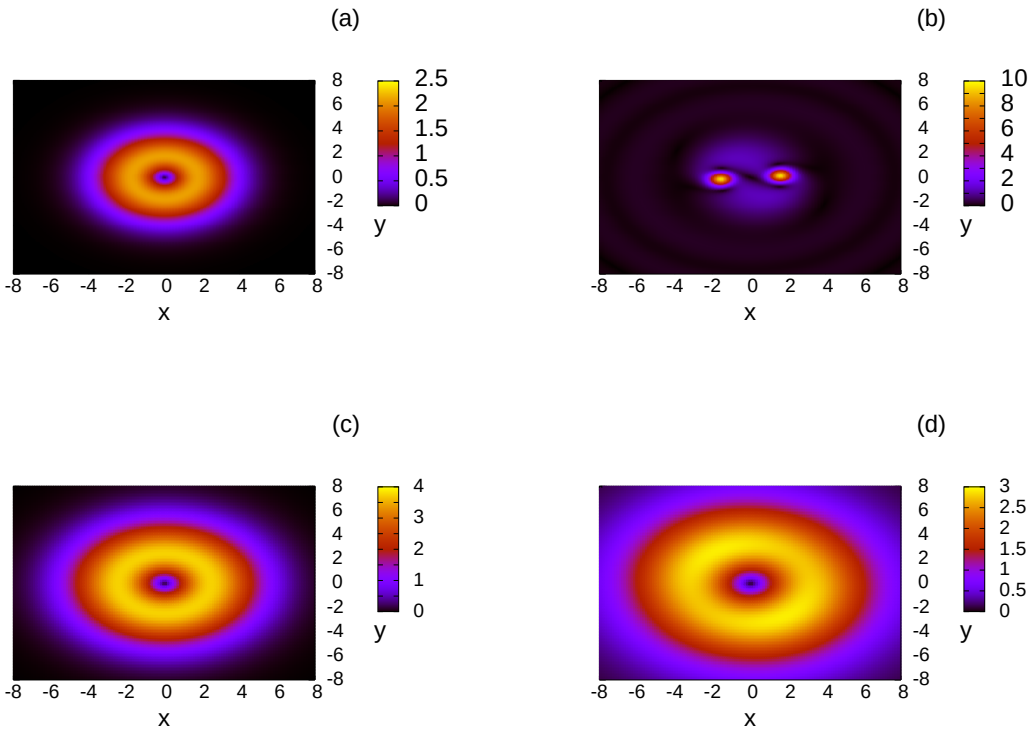

Figure 4: Numerical solutions of nematic equations (15) and (16) for $|u|$ for the vortex initial condition (70). (a) Initial local vortex, $z = 0$, for $a = 2$, $w = 2.5$, $\nu = 0.5$, (b) local vortex at $z = 6$, (c) initial nonlocal vortex at $z = 0$, for $a = 2.5$, $w = 3.5$, $\nu = 200$, (d) nonlocal vortex at $z = 100$. Here $q = 2$.

evolved and expanded slightly to evolve to a steady state, but does not show the mode-2 azimuthal instability.

Optical vortex solitary waves are much more difficult to generate in NLC experiments than nematicons, mainly because for nematicons the cell is much larger in one transverse direction than the other. The drawback of this configuration is that the bounded NLC is not symmetric in the transverse directions, which prevents the formation of stable optical vortex solitary waves [201, 202]. As stated in Section 2, a typical nematic cell has a transverse width of $100\mu m$, but this width can be as low as $30\mu m$. This issue of transverse non-symmetry is then not important for nematicons as a typical nematicon has a $3\mu m$ waist [16], while it is important for a vortex as a vortex has a typical width of $20\mu m$. To overcome these obstacles and successfully generate stable optical vortices in nematic liquid crystals, bulk NLC samples without lateral boundaries and the molecular director preset by an external magnetic field [77] were successfully used [203]. In this manner, dimensional restrictions and the influence of non-symmetric boundary conditions were avoided, enabling the successful generation of stable vortex solitary waves.

The precise mechanism by which nonlocality stabilises optical vortices in nonlinear media, including nematic liquid crystals, has been studied using a number of methods, besides verification via numerical solutions, as in Figure 4. A standard linear stability analysis, based

on numerically evaluating the steady vortex solitary wave of the nematic equations (15) and (16), showed that a vortex is stable above a nonlocality threshold [170]. This stabilisation due to the nonlocal medium response was also shown using a Gaussian approximation to the real nematic response [204]. The modulation theory methods outlined in Section 4 give more insight into the actual stabilisation [205]. For a local medium, the response mirrors the light distribution, so that it is zero at the node of the vortex. In the limit $\nu \to 0$, the director equation (16) gives $\theta = |u|^2/q$, so that $\theta = 0$ when $u = 0$. The modulation theory analysis shows that when $\nu \neq 0$, the medium response does not vanish at the singularity. Indeed, if ν is large enough, the director response over the core is large and wide enough to stably support the optical vortex [205]. In addition to this physical explanation of the stabilising effect of the nonlocal response of the nematic medium on optical vortices, this modulation theory analysis also gives a stability threshold in the nonlocality parameter ν [205] which is in excellent agreement, within 10%, of the value from a linearised stability analysis [170].

The same stabilising mechanism can be exploited by co-propagating a nematicon coaxial with an optical vortex [206, 207], as recently demonstrated in standard NLC cells with incoherent input beams of distinct wavelengths [94, 208]. The co-propagating nematicon raises the nonlinear director response under the core of the vortex, stabilising it. This modulation theory analysis was extended to study the influence of boundaries on vortex stability [209], finding that the nonlocal response can suffice to stabilise the vortex, unless the vortex width is comparable with the size of the cell. In a similar manner, the medium nonlocality can also stabilise the interaction of optical vortices [210]. Finally, the stabilising influence of co-propagating coaxial nematicons caused by raising the director profile under the singularity (vortex core) can also stabilise optical vortices undergoing refraction through dielectric interfaces or in non-uniform environments [211, 212, 213].

6 Modelling Experiments

The control of nematicons and optical vortices through refractive index changes was described in general terms in the previous Section. An interesting example of nematicon trajectory design/control is its bending in non-uniform, bias-free NLC cells [62, 63, 107, 124]. We provide here the basic details and show how simple models can give both accurate predictions of the results and insight into the underlying mechanism.

Let us consider a planar cell as outlined in Section 3, without external bias, so that $q = 0$, and a non-uniform director distribution θ. Let us assume that the background orientation θ has a mean $\bar{\theta}$ and a variation θ_b about it which is a function of y in non-dimensional variables (or Y in dimensional variables). The varying background results in a non-uniform refractive index and walk-off, so that a nematicon propagating in the sample moves along a non-straight path. The non-dimensional equations governing nematicon propagation in non-uniform NLC are as in Section 3, (10) and (11), but with θ replaced by $\bar{\theta}$ in (9) and in the dimensionless parameters (12) and (13). They are

$$i\frac{\partial u}{\partial z} + i\gamma\Delta(\bar{\theta} + \theta_b(y))\frac{\partial u}{\partial y} + \frac{1}{2}\nabla^2 u + 2\left(\theta_b(y) + \phi\right)u = 0, \tag{71}$$

$$\nu\nabla^2\phi = -2|u|^2, \tag{72}$$

The extra term θ_b arises from the expansion of the trigonometric function $\sin(\theta + \phi) =$

$\sin(\bar{\theta}+\theta_b+\phi)$ in the dimensional equation (6). The Lagrangian for these equations is

$$L = i\left(u^*u_z - uu_z^*\right) + i\gamma\Delta(\bar{\theta}+\theta_b)\left(u^*u_y - uu_y^*\right) - |\nabla u|^2 + 4\left(\theta_b+\phi\right)|u|^2 - \nu|\nabla\phi|^2, \quad (73)$$

As there are no known general nematicon solutions upon which to base standard solitary wave perturbation theory, the generalised modulation theory, variational approximations, as outlined in Section 4 need to be used. To this end, since the NLC medium is slowly varying, specific profiles for the nematicon and the director distribution need not be assumed to obtain modulation equations for the pertinent parameters [62, 63, 107]. Let us then set the nematicon and director distribution to have the forms

$$u = af_e(\rho)e^{i\sigma+iV(y-\xi)} \quad \text{and} \quad \phi = \alpha f_d(\mu), \quad (74)$$

where

$$\rho = \frac{\sqrt{x^2+(y-\xi)^2}}{w}, \quad \mu = \frac{\sqrt{x^2+(y-\xi)^2}}{\beta}. \quad (75)$$

Here f_e and f_d are the unknown profiles of the electric field of the beam and the director orientation, respectively. Substituting these general profiles into the Lagrangian (73) and averaging by integrating in x and y from $-\infty$ to ∞ gives the averaged Lagrangian

$$\begin{aligned}\mathcal{L} &= -2S_2\left(\sigma' - V\xi'\right)a^2w^2 - S_{22}a^2 - S_2\left(V^2+2VF_1-4F\right)a^2w^2 + \alpha a^2w^2S_m \\ &\quad - 4\nu S_{42}\alpha^2, \end{aligned} \quad (76)$$

where prime denotes differentiation with respect to z. Here F and F_1, determining the beam trajectory, are expressed by

$$F(\xi) = \frac{\int_{-\infty}^{\infty}\int_{-\infty}^{\infty}\theta_b f_e^2\,dxdy}{\int_{-\infty}^{\infty}\int_{-\infty}^{\infty}f_e^2\,dxdy}, \quad (77)$$

$$F_1(\xi) = \frac{\int_{-\infty}^{\infty}\int_{-\infty}^{\infty}\gamma\Delta\left(\bar{\theta}+\theta_b\right)f_e^2\,dxdy}{\int_{-\infty}^{\infty}\int_{-\infty}^{\infty}f_e^2\,dxdy}. \quad (78)$$

The integrals S_2, S_m, S_{22} and S_{42} appearing in $\mathcal{L}$ are

$$\begin{aligned} S_2 &= \int_0^\infty \zeta f_e^2(\zeta)\,d\zeta, \quad S_{22} = \int_0^\infty \zeta f_e'^2(\zeta)\,d\zeta, \\ S_m &= \int_0^\infty f_d(w\zeta/\beta)f_e^2(\zeta)\,d\zeta, \quad S_{42} = \frac{1}{4}\int_0^\infty \zeta\left[\frac{d}{d\zeta}f_d(\zeta)\right]^2 d\zeta. \end{aligned} \quad (79)$$

Their exact values are unnecessary in order to determine the curved trajectories.

Taking variations of (76) with respect to velocity V and position ξ gives the modulation equations

$$\frac{d}{dz}a^2w^2V = \left[2\frac{dF}{d\xi} - V\frac{dF_1}{d\xi}\right]a^2w^2, \quad (80)$$

$$\frac{d\xi}{dz} = V + F_1, \quad (81)$$

which yield the nematicon trajectory in the non-uniform medium. We note that the variational equation (80) is the same as Newton's Second Law for a particle of mass a^2w^2 travelling at

velocity V acted on by a force $[2F_\xi - VF_{1\xi}]\, a^2w^2$, so it is a "momentum" equation. In the present optical context, a^2w^2 is the power. In principle, these momentum equations need to be complemented by modulation equations for the beam amplitude and width obtained by variations of the averaged Lagrangian (76) with respect to the other parameters. However, these are not needed as the nonlocality ν is large, therefore the beam sheds diffractive radiation of very low amplitude on a very long z scale as it evolves [145]. Hence, the beam power a^2w^2 can be taken constant and the momentum equation (80) becomes

$$\frac{dV}{dz} = 2\frac{dF}{d\xi} - V\frac{dF_1}{d\xi}. \tag{82}$$

The integrals F (77) and F_1 (78) involve the beam profile f_e but, again, its details are not required. We note that $\bar\theta$ is a constant, whereas— of critical importance— θ_b is slowly varying relative to the beam width, typically $\theta_b' \sim 0.002\,\mathrm{rad}/\mu\mathrm{m}$ [62, 107]. A typical length scale for the varying background orientation is 500 μm, while a typical beam size is a few μm. The key momentum integrals (77) and (78) can thus be approximated by

$$\begin{aligned} F(\xi) &\sim \theta_b(\xi), \\ F_1(\xi) &\sim \gamma\Delta(\bar\theta + \theta_b(\xi)) = \gamma\Delta(\bar\theta) + \gamma\Delta'(\bar\theta)\theta_b(\xi) + \ldots, \end{aligned} \tag{83}$$

so that the momentum equations (81) and (82) become

$$\frac{dV}{dz} = \left(2 - V\gamma\Delta'(\bar\theta)\right)\theta_b'(\xi), \tag{84}$$

$$\frac{d\xi}{dz} = V + \gamma\Delta(\bar\theta) + \gamma\Delta'(\bar\theta)\theta_b(\xi). \tag{85}$$

These can be integrated to obtain the nematicon trajectory ξ given the background orientation variation $\bar\theta + \theta_b$.

Experiments [62] on nematicon bending were carried out in planar cells with a pre-imposed linear director variation (through anchoring at the interfaces) in the transverse direction Y. Hence, we take

$$\bar\theta = \frac{1}{2}(\theta_i + \theta_L), \quad \theta_b(y) = \frac{\theta_L - \theta_i}{L}y + \frac{1}{2}\left(\theta_i - \theta_L\right). \tag{86}$$

For such a linear variation, the momentum equations (84) and (85) have the exact solution

$$\xi = \left[\xi_0 + \frac{1 + \gamma^2\Delta'(\bar\theta)\Delta(\bar\theta)}{\gamma^2\Delta'^2(\bar\theta)\theta_b'}\right] e^{\gamma\Delta'(\bar\theta)\theta_b' z} - \frac{2 + \gamma^2\Delta'(\bar\theta)\Delta(\bar\theta)}{\gamma^2\Delta'^2(\bar\theta)\theta_b'} + \frac{1}{\gamma^2\Delta'^2(\bar\theta)\theta_b'} e^{-\gamma\Delta'(\bar\theta)\theta_b' z} \tag{87}$$

as θ_b' is a constant. Comparisons between this exact prediction and the experimentally acquired paths [62] are shown in Figure 5 for various input positions corresponding to different director orientation angles at the beam input. The agreement is very good, especially in light of the simplifications leading to the momentum equations (84) and (85). We thus see that simple momentum conservation allows for excellent agreement with measured results. Conversely, the approximation discloses the simple mechanism of momentum conservation behind the actual physics. A similar analysis of nematicon curvature in an NLC cell with a longitudinal Z variation of the background orientation θ can be conducted, that is singling out the role of walk-off variations without refraction: again, the agreement between the modelling and the experimental results is excellent [63], see Fig. 6 for a typical comparison between experimental and modulation theory results.

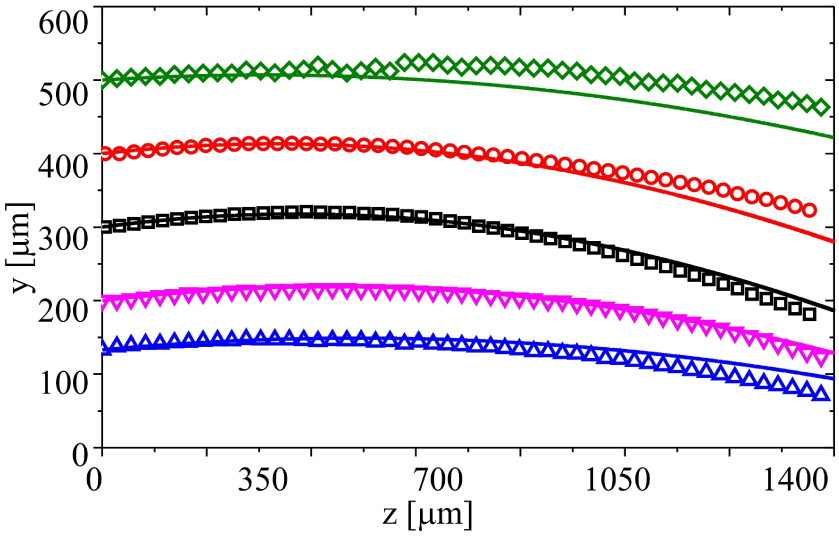

Figure 5: Nematicon trajectories— measured experimentally and calculated using modulation theory (87)— in an NLC sample non-uniform in the transverse Y coordinate. The background varies linearly from $\theta = 90^o$ at $Y = 0\mu m$ to $\theta = 0^o$ at $Y = 600\mu m$. Measured data: symbols; dynamical equations: lines. The input is a $3mW$ Gaussian beam of waist $3\mu m$ and wavelength $1.064\mu m$. Results reproduced from [62].

The modelling of experimental measurements can be illustrated in another non-uniform NLC environment [214]. In this example, a wide waveguide is induced by an external electric field (voltage) applied through straight electrodes and invariant along Z, with a non-uniform transverse distribution, as illustrated in Figure 7. At low beam powers the electric potential traps a nematicon in the gap region (waveguide) between the electrodes. However, a nematicon is a nonlinear wavepacket and so can change its environment, in particular the director distribution, so that the local refractive index gets altered. At high enough beam powers this refractive index increase can be large enough to overcome the externally imposed potential well and let the nematicon escape, that is tunnel out of the waveguide, as illustrated in Figure 8. While the NLC sample and the detailed experimental configuration were complicated by a resulting tilt of the optic axis out of the principal plane (Y, Z), this nematicon tunnelling can be simply modelled based on the momentum equation for the beam [108]. The effect of the external, non-uniform electric field on the equations (10) and (11) is a background refractive index well $m(y)$ for the envelope equation and a pre-tilt parameter q becoming a function of y. This gives a local change θ_1 in the background director orientation from the uniform value θ_0 away from the electric bias. The non-dimensional equations governing nematicon tunnelling are then [108]

$$i\frac{\partial u}{\partial z} + \frac{1}{2}\nabla^2 u + 2\phi u + m(y)u = 0, \tag{88}$$

$$\nu\nabla^2\phi - 2q(y)\phi = -2|E|^2. \tag{89}$$

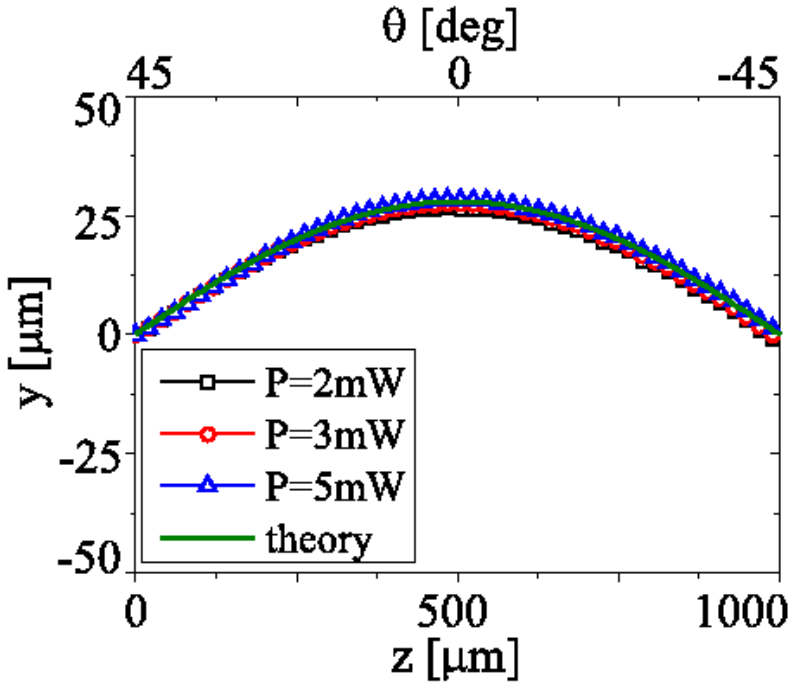

Figure 6: Comparisons between modulation theory and experimental results for nematicon trajectories in a non-uniform cell with background angle θ varying linearly in Z from 45^o at $z = 0mm$ to -45^o at $Z = 1500mm$ for various powers P. Figure from [63].

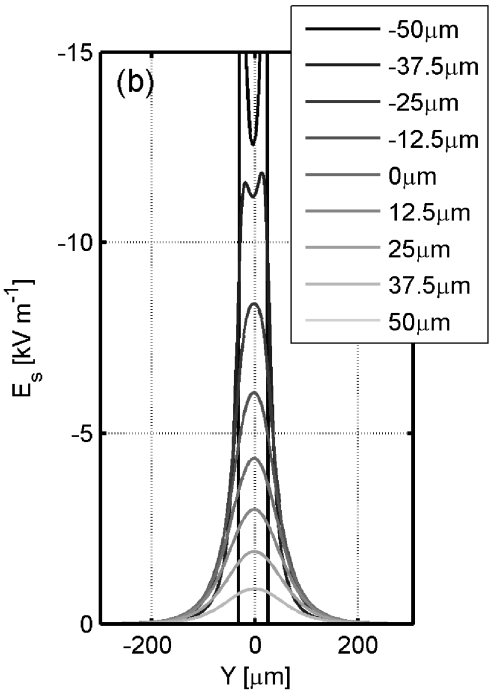

Figure 7: Y component of the static electric field E_s at different altitudes X across the NLC thickness, from $X = -50\mu m$ to $X = 50\mu m$. The vertical dashed lines indicate the edges of the two top electrodes for the applied voltage bias. Figure reproduced from [214].

Here, the key y-dependent parameters q and m stemming from the bias are

$$q(y) = \frac{4\Delta\epsilon_{RF}|\cos 2\theta_0|}{\epsilon_0 \Delta\epsilon \mathcal{E}^2 \sin 2\theta_0} E_s^2(y), \quad m(y) = \frac{2n_e^2(y)}{n_e^2(\theta_0)\Delta\epsilon \sin 2\theta_0}. \tag{90}$$

To determine the refractive index well $m(y)$ we use the extra-ordinary refractive index n_e from (1) and write

$$n_e = n_1(1 + n_2\theta_1), \tag{91}$$

where

$$n_1 = \frac{n_\perp n_\parallel}{\sqrt{n_\parallel^2 \cos^2\theta_0 + n_\perp^2 \sin^2\theta_0}} \quad \text{and} \quad n_2 = \frac{\left(n_\parallel^2 - n_\perp^2\right)\sin 2\theta_0}{2\left(n_\parallel^2 \cos^2\theta_0 + n_\perp^2 \sin^2\theta_0\right)}. \tag{92}$$

To complete the description we need the angle change θ_1 due to the external trapping electric field. The actual electric field forming the potential well, shown in Figure 7, is complicated, particularly towards its edges. For simplicity, a parabolic profile

$$E_s^2(y)/\mathcal{E}^2 = \gamma_2\left(L^2 - y^2\right), \tag{93}$$

for $-L \le y \le L$ was assumed, so that at $y = \pm L$ the electric field essentially vanishes. Hence, the background orientation resulting from this bias can, in principle, be calculated from the director equation (89) with $u = 0$. However, the resulting equation is a form of the parabolic cylinder equation [154], not useful to evaluate the integrals in the momentum

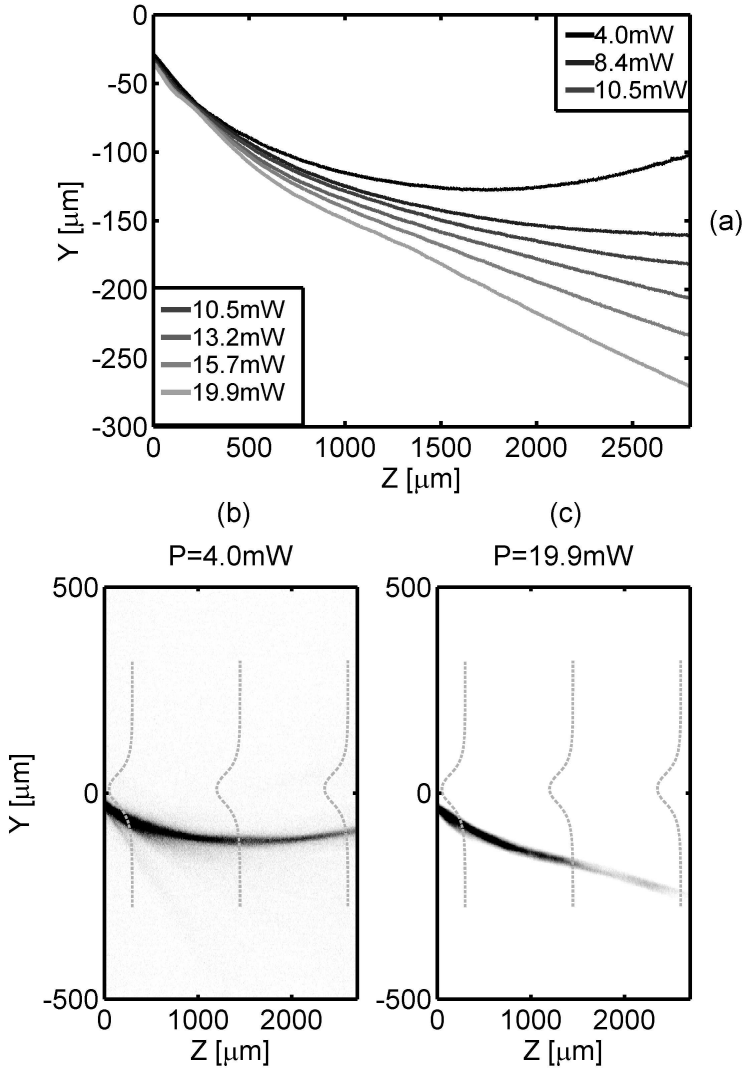

Figure 8: Sample data from experiments on nematicons ($\lambda = 1064nm$) escaping a wide waveguide induced by the external electric field as shown in Fig. 7. (a) Mean nematicon path for various input beam excitations: at low power the nematicons are trapped in the potential, whereas for $P > 15mW$ their initial momentum permits them to escape the potential. (b)–(c) Acquired photographs showing the evolution of a nematicon in the voltage-defined guiding profile for an input beam power of (b) 4.0 and (c) $19.9mW$, respectively. The latter case is that of a nematicon tunneling out. Figure reproduced from [214].

equation (95). To overcome this, the director angle change due to the potential well was taken to be parabolic, corresponding to Taylor expanding the parabolic cylinder function solution [108, 146]. Then

$$\theta_1 = \frac{\theta_c}{L^2}\left(L^2 - y^2\right), \tag{94}$$

where θ_c is the value of θ_1 on the waveguide axis $y = 0$.

It can be directly derived from the electric field equation (88) that the integrated equation for the beam momentum $i(u^* u_z - u u_z^*)$ is

$$i\frac{d}{dz}\int_{-\infty}^{\infty}\int_{-\infty}^{\infty}\left(u^* u_y - u u_y^*\right)\, dxdy = \int_{-\infty}^{\infty}\int_{-\infty}^{\infty}\left(-2|u|^2 m_y + 2\phi^2 q_y\right)\, dxdy. \tag{95}$$

Unfortunately, at this point general profiles for the nematicon cannot be used to determine trajectory equations from the momentum equation (95), as for the previous comparison with experimental results. At variance with the previous example of nematicon propagation in a non-uniform bias-free nematic cell, specific Gaussian profiles

$$u = ae^{-\left[x^2+(y-\xi)^2\right]/w^2} e^{i\sigma z + iV(y-\xi)} \quad \text{and} \quad \phi = \alpha e^{-\left[x^2+(y-\xi)^2\right]/\beta^2} \tag{96}$$

were chosen. Substituting these into the integral momentum conservation (95) results in the momentum equation

$$\frac{dV}{dz} = \frac{d^2\xi}{dz^2} = \left[2q_c\gamma_2\frac{\alpha^2\beta^2}{a^2w^2} - \frac{8n_2\theta_c}{\Delta\epsilon L^2\sin 2\theta_0}\right]\xi, \quad q_c = \frac{4\Delta\epsilon_{RF}}{\epsilon_0 n_a^2\mathcal{E}^2\tan 2\hat{\theta_0}}, \tag{97}$$

which determines the nematicon trajectory in the potential well. This differential equation can be integrated once to give

$$\left(\frac{d\xi}{dz}\right)^2 = V_0^2 + \left[2q_c\gamma_2\frac{\alpha^2\beta^2}{a^2w^2} - \frac{8n_2\theta_c}{\Delta\epsilon L^2\sin 2\theta_0}\right]\left(\xi^2 - \xi_0^2\right), \tag{98}$$

where ξ_0 and V_0 are the input beam position and angle, respectively. This trajectory equation allows the determination of the required nematicon power to escape the potential. The nematicon will just escape when the turning point of its trajectory $\xi' = 0$ occurs at the edge $\xi = L$ of the waveguide. The equation (98) gives the trajectory turning point ξ_t as

$$\xi_t^2 = \frac{V_0^2 + \left(\frac{8n_2\theta_c}{\Delta\epsilon L^2\sin 2\theta_0} - 2q_c\gamma_2\frac{\alpha^2\beta^2}{a^2w^2}\right)\xi_0^2}{\frac{8n_2\theta_c}{\Delta\epsilon L^2\sin 2\theta_0} - 2q_c\gamma_2\frac{\alpha^2\beta^2}{a^2w^2}}. \tag{99}$$

The nematicon tunnels out if $\xi_t > L$. The experimental parameters of [214], detailed in [108], yield an escape (critical) power $P_c = 18.7mW$ for a waveguide of effective width $200\mu m$, matching well with the measured range 16–$18mW$ [214].

Driven by the lack of exact solutions of the basic nematic equations (10) and (11), the two examples above demonstrate how simple modelling based on the underlying physics can produce excellent agreement with experimental results. As for the particle approximations of Section 4, it is apparent that basic concepts from classical mechanics, such as mass, momentum and energy conservation, are extremely useful in developing these models. The essential ingredient for these simple approximations to be successful in NLC is the material nonlocality. This nonlocal response acts as a trapping potential, permitting only weak leakage of the diffractive radiation shed as nonlinear beams, nematicons or vortices, evolve during propagation [124, 145].

7 Thermal Effects

The propagation of light beams in NLC can also be affected by thermal heating, not yet addressed in this paper with reference to extra-ordinary wave nematicons. In standard, undoped nematic liquid crystals, such as 5CB or E7, the single-photon absorption coefficient α is small, less than $0.2cm^{-1}$ [22, 23]. Nevertheless, thermal heating can be important for two reasons, (i) the refractive index eigenvalues $n_\perp$ and $n_\parallel$ and the walk-off δ are temperature dependent [22, 23, 24, 215, 216] and (ii) the nematic metaphase exists in a restricted temperature interval [14]. NLC thermal absorption can be enhanced or tailored at specific wavelengths or spectral ranges by the addition of absorbing dyes [25] or nano-particles [26] to increase energy withdrawal from the light beam. Since the intensity of the beam is $|A|^2$, the temperature is governed by the steady, forced heat equation

$$\kappa\nabla^2 T = -\alpha\Gamma|A|^2. \tag{100}$$

Here, as stated, α is the thermal absorption coefficient and κ the thermal conductivity. If we set T_0 to be a reasonable temperature increase and non-dimensionalise the temperature by $T = T_0 Q$, the non-dimensional temperature equation in the variables (8) is

$$\mu\nabla^2 Q = -|u|^2, \tag{101}$$

where the non-dimensional thermal conductivity is

$$\mu = \frac{\kappa T_0}{\alpha\Gamma W^2\mathcal{E}^2}. \tag{102}$$

It should be noted that, as the NLC parameters become temperature-dependent, a "typical" temperature $T_{\rm typ}$ has to be chosen and the parameters (9) have to be referred to $T_{\rm typ}$. The non-dimensional nematic system then becomes

$$i\frac{\partial u}{\partial z} + i\gamma\Delta\frac{\partial u}{\partial x} + \frac{1}{2}\nabla^2 u + 2\frac{\Delta\epsilon}{(\Delta\epsilon)_{\rm typ}}\phi u = 0, \tag{103}$$

$$\nu\nabla^2\phi - 2q\phi = -2\frac{\Delta\epsilon}{(\Delta\epsilon)_{\rm typ}}|u|^2, \tag{104}$$

with $\Delta\epsilon$, the walk-off Δ, the parameters ν and q being temperature-dependent.

In common NLC the thermo-optic refractive response is self-defocusing for extra-ordinary waves, opposite to the reorientation. These two contributions therefore counteract one another, i.e., they compete [24, 215, 216]. The thermal dependence of the refractive indices $n_\perp$ and $n_\parallel$ are non-trivial, but can be well approximated by cubics, except near the transition temperature where the material changes phase and becomes isotropic [14, 216].

A major effect of these competing reorientational and thermal nonlinearities is on the form of the nematicon [104, 217]. The former tends to hold the nematicon together through focusing, while the latter tends to pull the solitary wave apart. In some cases, when the two nonlinearities are carefully tailored by the introduction of dopants and specific wavelengths are employed, the $(1+1)$-dimensional nematicon solution becomes two-humped, resembling a "volcano" [104]. This "volcano" nematicon also arises from variational approximations whereby the true response kernel in the nonlocal form (30) of the nematic equations is replaced by a Gaussian [217]. The effect of a thermo-optic refractive response on optical vortex stability

has also been investigated for the nematic liquid crystal 6CHBT [218]. The defocusing thermal response was found to enhance the stability of an optical vortex, although, due to the small thermal absorption of 6CHBT, this effect is small, but can be enhanced by the addition of dyes to the nematic [218]. The physical reason for the thermal enhancement of stability is broadly similar to the nonlocal stability enhancement discussed in Section 5. The thermo-optical response is defocusing, which broadens the beam and the resultant nematic response, so that the director response over the vortex core is enhanced, thus helping to stabilise the vortex.

The opposite signs of the competing responses also affect nematicon interactions. At low powers and low heating, reorientation dominates and the interaction is attractive (as usual for nematicons [51] and for in-phase NLS solitons [7]); at high powers and high heating, the interaction is repulsive [105] (as for out of phase NLS solitons [7]). Variational methods based on a Gaussian for G in (30), as well as the Snyder-Mitchell approximation [42], can be used to predict this temperature dependent interaction of nematicons [219]. For a high power nematicon of sufficient "mass", in analogy with Kerr-like solitary waves [3, 7], it will split into multiple nematicons as the thermal defocusing causes the wavepackets to repel each other and propagate with opposite transverse velocities from the "volcano's crater" (intensity minimum) [113].

The thermo-optic response via absorbed beam power changes the NLC indices and birefringence, so it can also have significant effects on nematicon trajectories through the walkoff, and on solitary wave confinement through the index contrast. It also perturbs the elastic constant(s) and the effective nonlocality/nonlinearity [25, 101, 216, 220]. Such beam self-induced changes are weak in standard NLC, with trajectories being altered by angles of the order of degrees [216].

The study of temperature-dependent NLC properties on the formation and propagation of reorientational optical solitary waves is recent and many issues are still open, particularly analytical studies, especially in the experimental domain of $(2 + 1)$ dimensions. Conversely, it deserves mentioning— in closing this Section— that early work on beam self-focusing and "quasi-solitons" in nematic liquid crystals was indeed based on light absorption in dye-doped samples in capillaries or planar cells, although the experimental observations, because of their pioneering character, did not exhaustively address the various optical aspects of the nonlinear phenomena: polarization, nonlocality and dissipation [30, 32, 33, 221]. The lack of well-defined pre-treated input interfaces to the samples introduced the possibility of air/NLC menisci, with the risk of beam depolarization and subsequent polarization evolution from linear to elliptic, circular, etc. The large amount of dopants, aimed at increasing the nonlinear response through the Janossy effect [221, 222], also increased the propagation losses and the heating, with detrimental effects on the order parameter, as well as causing fluid convection, particularly when employing continuous wave lasers at visible wavelengths. The inclusion of fluid motion with the nonlinear optics of the nematic introduces a whole new level of complexity, particularly as nematics are non-Newtonian fluids. Beam filamentation, undulation and self-collimation have been observed and reported in cells with different anchoring at the boundaries [33, 223], including solitary waves generated by ordinary-wave input beams and isotropic channels beyond the nematic-isotropic transition [31, 99, 221, 224, 225]. In NLC the ordinary-wave refractive index eigenvalue, in fact, is a growing function of temperature in the nematic phase [13] and can therefore support self-focusing via a thermo-optic response in absorbing mixtures, counteracting diffraction and undergoing no Poynting-vector walkoff.

8 Conclusions

Nematic liquid crystals are an ideal medium/platform for the study of propagating nonlinear dispersive optical wavepackets, including the standard example of optical solitary waves, termed nematicons. Light beam propagation in nematic liquid crystals constitutes an ideal environment for many of the ideas and techniques developed since the 1960s for the study of nonlinear dispersive waves. However, as the nematic equations are a coupled system of an NLS-type equation for the beam and an elliptic equation for the medium response, this added complexity means that no exact, general solutions have been derived to date. Several standard techniques for analysing nonlinear waves, such as inverse scattering, perturbed solitary wave theory and Whitham modulation theory, are then unavailable. Despite such a difficulty, the study of light beams in NLC has prompted the development of modified and sometimes sophisticated new approaches. Numerical techniques, whether to solve the reduced equations (10) and (11) [21, 20] or the full vectorial Maxwell and director equations [46] are available and can confirm/verify the accuracy of solutions obtained using approximations. However, while solving the full vectorial equations is computationally expensive and time consuming, numerical solutions of the reduced equations do not provide the physical and mathematical insight available from analytical solutions, particularly when experimental data can benefit from analytical results to gain insight into the underlying mechanisms, as seen, e.g., in Section 6.

Compiling the state of the art and illustrating the main aspects related to the modelling of self-confined optical solitary waves in nematic liquid crystals, this overview has hopefully shown that this NLC niche in the optics, physics and mathematics of nonlinear waves has been and continues to be a rather active contemporary theme of research, with numerous aspects of applied relevance into the diverse areas where nonlinear dispersive waves were first discovered and later investigated, from fluid/atmosphere/ocean waves to plasmas and biology and more [3, 8, 9].

References

[1] Sir H. Lamb, *Hydrodynamics,* Dover Publications Inc., New York (1932).

[2] J.S. Russell, "Report on waves," *14th meeting of the British Association for the Advancement of Science,* John Murray, London, 311–390 (1845).

[3] G.B. Whitham, *Linear and Nonlinear Waves,* J. Wiley and Sons, New York (1974).

[4] J. Boussinesq, "Théorie de l'intumescence liquide appelée onde solitaire ou de translation se propageant dans un canal rectangulaire," *Comptes Rendus,* **72**, 755–759 (1871).

[5] D.J. Korteweg and G. de Vries, "On the change of form of long waves advancing in a rectangular channel, and on a new type of long stationary waves," *Phil. Mag.,* **39**, 422–443 (1895).

[6] C.S. Gardner, J. M. Greene, M. D. Kruskal and R. M. Miura, "Method for solving the Korteweg-deVries equation," *Phys. Rev. Lett.,* **19**, 1095–1097 (1967).

[7] A.C. Newell, *Solitons in Mathematics and Physics,* SIAM, Philadelphia (1985).

[8] M.J. Ablowitz, *Nonlinear Dispersive Waves. Asymptotic Analysis and Solitons,* Cambridge University Press, Cambridge (2011).

[9] A.S. Davydov, *Solitons in Molecular Systems, 2nd ed.,* Kluwer Academic Publishers, Dordrecht (1991).

[10] G.B. Whitham, "Non-linear dispersive waves," *Proc. Roy. Soc. Lond. A— Math. Phys. Sci.,* **283**, 238–261 (1965).

[11] G.A. El and M.A. Hoefer, "Dispersive shock waves and modulation theory," *Physica D,* **333**, 11–65 (2016).

[12] P.-G. De Gennes, *The Physics of Liquid Crystals,* Clarendon Press, Oxford (1979).

[13] I. C. Khoo and S. T. Wu, *Optics and Nonlinear Optics of Liquid Crystals,* World Scientific, Singapore (1993).

[14] I.C. Khoo, *Liquid Crystals: Physical Properties and Nonlinear Optical Phenomena,* Wiley, New York (1995).

[15] M. Peccianti, A. De Rossi, G. Assanto, A. De Luca, C. Umeton and I. C. Khoo, "Electrically assisted self-confinement and waveguiding in planar nematic liquid crystal cells," *Appl. Phys. Lett.,* **77**, 7–9 (2000).

[16] M. Peccianti and G. Assanto, "Nematicons," *Phys. Rep.,* **516**, 147–208 (2012).

[17] Y.S. Kivshar and G.P. Agrawal, *Optical Solitons. From Fibers to Photonic Crystals,* Academic Press, San Diego (2003).

[18] M. Peccianti, C. Conti and G. Assanto, "The interplay between nonlocality and nonlinearity in nematic liquid crystals," *Opt. Lett.,* **30**, 415–417 (2005).

[19] C. Conti, M. Peccianti and G. Assanto, "Observation of optical spatial solitons in a highly nonlocal medium," *Phys. Rev. Lett.,* **92**, 113902 (2004).

[20] B. Fornberg and G.B. Whitham, "Numerical and theoretical study of certain non-linear wave phenomena," *Phil. Trans. Roy. Soc. Lond. Ser. A— Math. and Phys. Sci.,* **289**, 373–404 (1978).

[21] T.F. Chan and T. Kerkhoven, "Fourier methods with extended stability intervals for KdV," *SIAM J. Numer. Anal.,* **22**, 441–454 (1985).

[22] I.C. Khoo, "Nonlinear optics, active plasmonics and metamaterials with liquid crystals," *Prog. Quantum Elect.,* **38**, 77–117 (2014).

[23] I.C. Khoo, S. Webster, S. Kubo, W. J. Youngblood, J. Liou, A. Diaz, T. E. Mallouk, P. Lin, D. Peceli, L.A. Padilha, D.J. Hagan and E.W. Van Stryland, "Synthesis and characterization of the multi-photon absorption and excited-state properties of 4-propyl 4'-butyl diphenyl acetylene," *J. Mater. Chem.,* **19**, 7525–7531 (2009).

[24] L. Abdulkareem, S.F. Abdalah, K. Al Maimee and R. Meucci, "Temperature effect on nonlinear refractive indices of liquid crystals in visible and NIR," *Opt. Commun.,* **363**, 188–194 (2016).

[25] U.A. Laudyn, M. Kwasny, A. Piccardi, M.A. Karpierz, R. Dabrowski, O. Chonjowska, A. Alberucci and G. Assanto, "Nonlinear competition in nematicon propagation," *Opt. Lett.,* **40**, 5235–5238 (2015).

[26] M.Y. Salazar-Romero, Y.A. Ayala, E. Brambila, L.A. Lopez-Peña, L. Sciberras, A.A. Minzoni, R.A. Terborg, J.P. Torres and K. Volke-Sepúlveda, "Steering and switching of soliton-like beams via interaction in a nanocolloid with positive polarizability," *Opt. Lett.,* **42**, 2487–2490 (2017).

[27] N. V. Tabiryan, A. V. Sukhov and B. Ya. Zel'dovich, "Orientational optical nonlinearity of liquid crystals," *Mol. Cryst. Liq. Cryst.,* **136**, 1–139 (1986).

[28] M. Peccianti and G. Assanto, "Nematic liquid crystals: a suitable medium for self-confinement of coherent and incoherent light," *Phys. Rev. E,* **65**, 035603–035606 (2002).

[29] G. Assanto and M. Karpierz, "Nematicons: self-localized beams in nematic liquid crystals," *Liq. Cryst.,* **36**, 1161–1172 (2009).

[30] E. Braun, L. Faucheux, A. Libchaber, D.W. McLaughlin, D.J. Muraki and M.J. Shelley, "Filamentation and undulation of self-focused laser beams in liquid crystals," *Europhys. Lett.,* **23**, 239–244 (1993).

[31] M. Warenghem, J.F. Henninot, F. Derrien and G. Abbate, "Thermal and orientational 2D+1 spatial optical solitons in dye doped liquid crystals," *Mol. Cryst. Liq. Cryst.,* **373**, 213–225 (2002).

[32] F. Derrien, J.F. Henninot, M. Warenghem and G. Abbate, "A thermal $(2D+1)$ spatial optical soliton in a dye doped liquid crystal," *J. Opt. A: Pure Appl. Opt.,* **2**, 332–337 (2000).

[33] M. Warenghem, J.F. Henninot and G. Abbate, "Non-linearly induced self waveguiding structure in dye doped nematic liquid crystals confined in capillaries," *Opt. Express,* **2**, 483–490 (1998).

[34] S. Slussarenko, A. Alberucci, C.-P. Jisha, P. Piccirillo. E. Santamato, G. Assanto and L. Marrucci, "Guiding Light via Geometric Phases," *Nat. Photon.,* **10**, 571–575 (2016).

[35] A. Alberucci, C. P. Jisha, L. Marrucci, and G. Assanto, "Electromagnetic confinement via Spin-Orbit interaction in anisotropic dielectrics," *ACS Photon.,* **3**, 2249–2254 (2016).

[36] M.A. Karpierz, M. Sierakowski, M. Swillo and T. Wolinski, "Self-focusing in liquid crystalline waveguides," *Mol. Cryst. Liq. Cryst.,* **320**, 157–163 (1998).

[37] M.A. Karpierz, "Solitary waves in liquid crystalline waveguides," *Phys. Rev. E.,* **66**, 036603 (2002).

[38] M. Kwasny, U. A. Laudyn, F.A. Sala, A. Alberucci, M.A. Karpierz and G. Assanto, "Self-guided beams in low-birefringence nematic liquid crystals," *Phys. Rev. A,* **86**, 01382 (2012).

[39] W. E. Torruellas, G. Assanto, B. L. Lawrence, R. A. Fuerst and G. I. Stegeman, "All-optical switching by spatial walk-off compensation and solitary-wave locking," *Appl. Phys. Lett.,* **68**, 1449–1451 (1996).

[40] D.J. Armstrong, W.J. Alford, T.D. Raymond, A.V. Smith and M.S. Bowers, "Parametric amplification and oscillation with walkoff-compensating crystals," *J. Opt. Soc. Amer. B,* **14**, 460–474 (1997).

[41] G. Assanto, "Nematicons: reorientational solitons from optics to photonics," *Liq. Cryst. Rev.,* **6**, 170–194 (2018).

[42] A.W. Snyder and M.J. Mitchell, "Accessible solitons," *Science,* **276**, 1538–1541 (1997).

[43] A. Alberucci, A. Piccardi, M. Peccianti, M. Kaczmarek and G. Assanto, "Propagation of spatial optical solitons in a dielectric with adjustable nonlinearity," *Phys. Rev. A,* **82**, 023806 (2010).

[44] A. Piccardi, A. Alberucci and G. Assanto, "Self-turning self-confined light beams in guest-host media," *Phys. Rev. Lett.,* **104**, 213904 (2010).

[45] G. Assanto and M. Peccianti, "Spatial solitons in nematic liquid crystals," *IEEE J. Quantum Electron.,* **39**, 13–21 (2003).

[46] G.D. Ziogos and E.E. Kriezis, "Modeling light propagation in liquid crystal devices with a 3-D full-vector finite-element beam propagation method," *Opt. Quantum Electron.,* **40**, 733–748 (2008).

[47] F.A. Sala and M.A. Karpierz, "Modeling of molecular reorientation and beam propagation in chiral and non-chiral nematic liquid crystals," *Opt. Express,* **20**, 13923–13928 (2012).

[48] F. Sala, N.F. Smyth, U. Laudyn, M.A. Karpierz, A.A. Minzoni and G. Assanto, "Bending reorientational solitons with modulated alignment," *J. Opt. Soc. Amer. B,* **34,** 2459–2466 (2017).

[49] C. Conti, M. Peccianti and G. Assanto, "Route to nonlocality and observation of accessible solitons," *Phys. Rev. Lett.,* **91**, 073901 (2003).

[50] S. Skupin, O. Bang, D. Edmundson and W. Krolikowski, "Stability of two-dimensional spatial solitons in nonlocal nonlinear media," *Phys. Rev. E,* **73**, 066603(2006).

[51] M. Peccianti, K.A. Brzdąkiewicz and G. Assanto, "Nonlocal spatial soliton interactions in bulk nematic liquid crystals," *Opt. Lett.,* **27**, 1460–1462 (2002).

[52] M. Peccianti, C. Conti, G. Assanto, A. De Lucam and C. Umeton, "All optical switching and logic gating with spatial solitons in liquid crystals," *Appl. Phys. Lett.,* **81**, 3335–3337 (2002).

[53] W. Hu, T. Zhang, Q. Guo, L. Xuan and S. Lan, "Nonlocality-controlled interactions of spatial solitons in nematic liquid crystals," *Appl. Phys. Lett.,* **89**, 071111 (2006).

[54] C. Conti, M. Peccianti and G. Assanto, "Complex dynamics and configurational entropy of spatial optical solitons in nonlocal media," *Opt. Lett.,* **31**, 2030–2032 (2006).

[55] A. Fratalocchi, A. Piccardi, M. Peccianti and G. Assanto, "Nonlinearly controlled angular momentum of soliton clusters," *Opt. Lett.,* **32**, 1447–1449 (2007).

[56] Y.Q. Zhu, X.W. Long, W. Hu, L.G. Cao, P.B. Yang and Q. Guo, "The influence of nonlocality on solitons in nematic liquid crystals," *Acta Phys. Sin.,* **57**, 2260–2265 (2008).

[57] W. Hu, S.G. Ouyang, P.B. Yang, Q. Guo and S. Lan, "Short-range interactions between strongly nonlocal solitons," *Phys. Rev. A,* **77**, 033842 (2008).

[58] Y. Izdebskaya, V. Shvedov, A.S. Desyatnikov, Y.S. Kivshar, W. Krolikowski and G. Assanto, " Incoherent interaction of nematicons in bias-free liquid crystal cells," *J. Eur. Opt. Soc.,* **5**, 10008 (2008).

[59] L.G. Cao, Y.J. Zheng, W. Hu, P.B. Yang and Q. Guo, "Long-range interactions between nematicons," *Chin. Phys. Lett.,* **26**, 064209 (2009).

[60] Y.V. Izdebskaya, V.G. Shvedov, A.S. Desyatnikov, W.Z. Krolikowski, M. Belic, G. Assanto and Y.S. Kivshar, "Counterpropagating nematicons in bias-free liquid crystals," *Opt. Express,* **18**, 3258–3263 (2010).

[61] M. Peccianti, C. Conti, G. Assanto, A.D. Luca and C. Umeton, "Routing of anisotropic spatial solitons and modulational instability in liquid crystals," *Nature,* **432**, 733–737 (2004).

[62] U.A. Laudyn, M. Kwaśny, F.A. Sala, M.A. Karpierz, N.F. Smyth and G. Assanto, "Curved optical solitons subject to transverse acceleration in reorientational soft matter," *Sci. Rep.,* **7**, 12385 (2017).

[63] U.A. Laudyn, M. Kwaśny, M. Karpierz, N.F. Smyth and G. Assanto, "Accelerated optical solitons in reorientational media with transverse invariance and longitudinally modulated birefringence," *Phys. Rev. A,* **98**, 023810 (2018).

[64] J. Beeckman, K. Neyts, P.J.M. Vanbrabant, R. James and F.A. Fernandez, "Finding exact spatial soliton profiles in nematic liquid crystals," *Opt. Express,* **18**, 3311–3321 (2010).

[65] M. Peccianti, A. Pasquazi, G. Assanto and R. Morandotti, "Enhancement of third harmonic generation in nonlocal spatial solitons," *Opt. Lett.,* **35**, 3342–3344 (2010).

[66] Y.V. Izdebskaya, A.S. Desyatnikov, G. Assanto and Y.S. Kivshar, "Multimode nematicon waveguides," *Opt. Lett.,* **36**, 184–186 (2011).

[67] S. Perumbilavil, A. Piccardi, R. Barboza, O. Buchnev, G. Strangi, M. Kauranen, and G. Assanto, "Beaming random lasers with soliton control," *Nature Commun.,* **9**, 3863 (2018).

[68] J.F. Henninot, J.F. Blach, and M. Warenghem, "Enhancement of dye fluorescence recovery in nematic liquid crystals using a spatial optical soliton," *J. Appl. Phys.,* **107**, 113111 (2010).

[69] S. Bolis, T. Virgili, S.K. Rajendran, J. Beeckman and P. Kockaert, "Nematicon-driven injection of amplified spontaneous emission into an optical fiber," *Opt. Lett.,* **41**, 2245–2248 (2016).

[70] A. Piccardi, U. Bortolozzo, S. Residori and G. Assanto, "Spatial solitons in liquid crystal light valves," *Opt. Lett.,* **34**, 737–739 (2009).

[71] A. Piccardi, A. Alberucci, U. Bortolozzo, S. Residori and G. Assanto, "Soliton gating and switching in liquid crystal light valve," *Appl. Phys. Lett.,* **96**, 071104 (2010).

[72] J. Beeckman, K. Neyts and M. Haelterman, "Patterned electrode steering of nematicons," *J. Opt. A: Pure Appl. Opt.,* **8**, 214–220 (2006).

[73] A. Piccardi, M. Peccianti, G. Assanto, A. Dyadyusha and M. Kaczmarek, "Voltage-driven in-plane steering of nematicons," *Appl. Phys. Lett.,* **94**, 091106 (2009).

[74] R. Barboza, A. Alberucci and G. Assanto, "Large electro-optic beam steering with nematicons," *Opt. Lett.,* **36**, 2611–2613 (2011).

[75] A. Piccardi, A. Alberucci, R. Barboza, O. Buchnev, M. Kaczmarek and G. Assanto, "In-plane steering of nematicon waveguides across an electrically adjusted interface," *Appl. Phys. Lett.,* **100**, 251107 (2012).

[76] Y. Izdebskaya, "Routing of spatial solitons by interaction with rod microelectrodes," *Opt. Lett.,* **39**, 1681–1684 (2014).

[77] Y. Izdebskaya, V. Shvedov, G. Assanto and W. Krolikowski, "Magnetic routing of light-induced waveguides," *Nature Commun.,* **8**, 14452 (2017).

[78] V. Shvedov, Y. Izdebskaya, Y. Sheng and W. Krolikowski, "Magnetically controlled negative refraction of solitons in liquid crystals," *Appl. Phys. Lett.,* **110**, ,091107 (2017).

[79] S. Perumbilavil, M. Kauranen and G. Assanto, "Magnetic steering of directional random laser in soft matter," *Appl. Phys. Lett.,* **113**, 121107 (2018).

[80] A. Piccardi, A. Alberucci and G. Assanto, "Soliton self deflection via power-dependent walk-off," *Appl. Phys. Lett.,* **96**, 061105 (2010).

[81] M. Peccianti, A. Dyadyusha, M. Kaczmarek and G. Assanto, "Tunable refraction and reflection of self-confined light beams," *Nature Phys.,* **2**, 737–742 (2006).

[82] M. Peccianti and G. Assanto, "Nematicons across interfaces: anomalous refraction and reflection of solitons in liquid crystals," *Opt. Express,* **15**, 8021–8028 (2007).

[83] A. Piccardi, A. Alberucci, N. Kravets, O. Buchnev and G. Assanto, "Power controlled transition from standard to negative refraction in reorientational soft matter," *Nat. Commun.,* **5**, 5533–5541 (2014).

[84] M. Peccianti, G. Assanto, A. Dyadyusha and M. Kaczmarek, "Non-specular total internal reflection of spatial solitons at the interface between highly birefringent media," *Phys. Rev. Lett.,* **98**, 113902 (2007).

[85] M. Peccianti, G. Assanto, A. Dyadyusha and M. Kaczmarek, "Nonlinear shift of spatial solitons at a graded dielectric interface," *Opt. Lett.,* **32**, 271–273 (2007).

[86] N. Kravets, A. Piccardi, A. Alberucci, A. Buchnev, M. Kaczmarek and G. Assanto, "Bistability with optical beams propagating in a reorientational mediuma," *Phys. Rev. Lett.,* **113**, 023901 (2014).

[87] A. Alberucci, A. Piccardi, N. Kravets and G. Assanto, "Beam hysteresis via reorientational self-focusing," *Opt. Lett.,* **30**, 5830–5833 (2014).

[88] J. M. L. MacNeil, N. F. Smyth and G. Assanto, "Exact and approximate solutions for optical solitary waves in nematic liquid crystals," *Physica D,* **284**, 1–15 (2014)

[89] A. Piccardi, N. Kravets, A. Alberucci, O. Buchnev and G. Assanto, "Voltage driven beam bistability in a reorientational uniaxial dielectric," *APL Photonics,* **1**, 011302 (2016).

[90] A. Alberucci, A. Piccardi, N. Kravets, O. Buchnev and G. Assanto, "Soliton enhancement of spontaneous symmetry breaking," *Optica,* **2**, 783–789 (2015).

[91] A. Fratalocchi, A. Piccardi, M. Peccianti and G. Assanto, "Nonlinearly controlled angular momentum of soliton clusters," *Opt. Lett.,* **32**, 1447–1449 (2007).

[92] A. Alberucci, M. Peccianti, G. Assanto, A. Dyadyusha and M. Kaczmarek, "Two-color vector solitons in non-local media," *Phys. Rev. Lett.,* **97**, 153903 (2006).

[93] G. Assanto, N.F. Smyth and A. L. Worthy, "Two color, nonlocal vector solitary waves with angular momentum in nematic liquid crystals," *Phys. Rev. A,* **78**, 013832 (2008).

[94] Y. V. Izdebskaya, G. Assanto and W. Krolikowski, "Observation of stable vector vortex solitons," *Opt. Lett.,* **40**, 4182–4185 (2015).

[95] U. Laudyn, M. Kwasny, M. Karpierz and G. Assanto, "Three-color vector nematicon," *Photon. Lett. Pol.,* **9**, 36–38 (2017).

[96] I. B. Burgess, M. Peccianti, G. Assanto and R. Morandotti, "Accessible light bullets via synergetic nonlinearities," *Phys. Rev. Lett.,* **102**, 203903 (2009).

[97] M. Peccianti, I. B. Burgess, G. Assanto and R. Morandotti, "Space-time bullet trains via modulation instability and nonlocal solitons," *Opt. Express,* **18**, 5934–5941 (2010).

[98] M. Warenghem, J.F. Blach and J.F. Henninot, "Thermo-nematicon: an unnatural coexistence of solitons in liquid crystals?," *J. Opt. Soc. Am. B,* **25**, 1882–1887 (2008).

[99] M. Warenghem, J.F. Blach and J.F. Henninot, "Measuring and monitoring optically induced thermal or orientational non-locality in nematic liquid crystal," *Mol. Cryst. Liq. Cryst.,* **454**, 297–314 (2006).

[100] U. A. Laudyn, M. Kwasny, A. Piccardi, M. Karpierz, R. Dabrowski, O. Chojnowska, A. Alberucci and G. Assanto, "Nonlinear competition in nematicon propagation," *Opt. Lett.,* **40**, 5235–5238 (2015).

[101] A. Alberucci, U. Laudyn, A. Piccardi, M. Kwasny, B. Klus, M. A. Karpierz and G. Assanto, "Nonlinear continuous-wave optical propagation in nematic liquid crystals: interplay between reorientational and thermal effects," *Phys. Rev. E,* **96**, 012703 (2017).

[102] S. Perumbilavil, A. Piccardi, O. Buchnev, G. Strangi, M. Kauranen and G. Assanto, "Spatial solitons to mold random lasers in nematic liquid crystals," *Opt. Mat. Express,* **8**, 3864–3878 (2018).

[103] U. Laudyn, A. Piccardi, M. Kwasny, M.A. Karpierz and G. Assanto, "Thermo-optic soliton routing in nematic liquid crystals," *Opt. Lett.,* **43**, 2296–2299 (2018).

[104] P. Jung, W. Krolikowski, U. Laudyn, M. Trippenbach and M.A. Karpierz, "Supermode spatial optical solitons in liquid crystals with competing nonlinearities," *Phys. Rev. A,* **95**, 023820 (2017).

[105] K. Cyprych, P. Jung, Y. Izdebskaya, D.N. Christodoulides and W. Krolikowski, "Anomalous interaction of spatial solitons in nematic liquid crystals," *Opt. Lett.,* **44**, 267–270 (2019).

[106] C. García-Reimbert, A.A. Minzoni, N.F. Smyth and A.L. Worthy, "Large-amplitude nematicon propagation in a liquid crystal with local response," *J. Opt. Soc. Amer. B,* **23**, 2551–2558 (2006).

[107] F.A. Sala, N.F. Smyth, U.A. Laudyn, M.A. Karpierz, A.A. Minzoni and G. Assanto, "Bending reorientational solitons with modulated alignment," *J. Opt. Soc. Amer. B,* **34**, 2459–2466 (2017).

[108] G. Assanto, A. A. Minzoni, M. Peccianti and N. F. Smyth, "Optical solitary waves escaping a wide trapping potential in nematic liquid crystals: modulation theory," *Phys. Rev. A,* **79**, 033837 (2009).

[109] N. Ghofraniha, C. Conti, G. Ruocco and S. Trillo, 2007, "Shocks in nonlocal media," *Phys. Rev. Lett.,* **99**, 043903.

[110] C. Rotschild, M. Segev, Z. Xu, Y.V. Kartashov and L. Torner, 2006, "Two-dimensional multipole solitons in nonlocal nonlinear media," *Opt. Lett.,* **31**, 3312–3314.

[111] C. Rotschild, B. Alfassi, O. Cohen and M. Segev, 2006, "Long-range interactions between optical solitons," *Nature Phys.,* **2**, 769–774.

[112] M. Segev, B. Crosignani, A. Yariv and B. Fischer, 1992, "Spatial solitons in photorefractive media," *Phys. Rev. Lett.,* **68**, 923–926.

[113] C.P. Jisha, J. Beeckman, F. van Acker, K. Neyts, S. Nolte and A. Alberucci, "Generation of multiple solitons using competing nonlocal nonlinearities," *Opt. Lett.,* **44**, 1162–1165 (2019).

[114] A. Cheskidov, D.D. Holm, E. Olson and E.S. Titi, 2005, "On a Leray-α model of turbulence," *Proc. R. Soc. Lond. A,* **461**, 629–649.

[115] A. Ilyin, E.M. Lunasin and E.S. Titi, 2006, "A modified-Leray-α subgrid scale model of turbulence," *Nonlinearity,* **19**, 879–897.

[116] R. Penrose, 1998, "Quantum computation, entanglement and state reduction," *Phil. Trans. R. Soc. Lond. A,* **356**, 1927–1939.

[117] I.M. Moroz, R. Penrose and P. Tod, "Spherically-symmetric solutions of the Schrödinger-Newton equations," *Classical and Quantum Gravity*, **15**, 2733–2742 (1998).

[118] A.H. Guth, M.P. Hertzberg and C. Prescod-Weinstein, "Do dark matter axions form a condensate with long-range correlation?", *Phys. Rev. D,* **92**, 103513 (2015).

[119] A. Paredes and H. Michinel, "Interference of dark matter solitons and galactic offsets," *Phys. Dark Universe,* **12**, 50–55 (2016).

[120] A. Navarrete, A. Paredes, J.R. Salgueiro and H. Michinel, "Spatial solitons in thermo-optical media from the nonlinear Schrödinger-Poisson equation and dark-matter analogues," *Phys. Rev. A,* **95**, 013844 (2017).

[121] A. Piccardi, A. Alberucci, N. Tabiryan and G. Assanto, "Dark nematicons," *Opt. Lett.,* **36**, 1356–1358 (2011).

[122] S.V. Serak, N.V. Tabiryan, M. Peccianti and G. Assanto, "Spatial soliton all-optical logic gates," *IEEE Photon. Technol. Lett.,* **18**, 1287–1289 (2006).

[123] G. Assanto, T.R. Marchant, A.A. Minzoni and N.F. Smyth, "Reorientational versus Kerr dark and grey solitary waves using modulation theory," *Phys. Rev. E,* **84**, 066602 (2011).

[124] G. Assanto, P. Panayotaros, and N. F. Smyth, "Mechanical analogies for nonlinear light beams in nonlocal nematic liquid crystals," *J. Nonl. Opt. Phys. Mat.,* **27**, 1850046 (2018).

[125] Y. Hu and Q. Zhu, "New analytic solutions of two-dimensional nonlocal nonlinear media, *Appl. Math. Comp.,* **305**, 53–61 (2017).

[126] S. Chandrasekar, *An Introduction to the Study of Stellar Structure,* Dover Publications, Mineloa, New York (2003).

[127] V.F. Zaitsev and A.D. Polyanin, *Handbook of Exact Solutions for Ordinary Differential Equations,* Chapman Hall/CRC Press (2002).

[128] D.E. Panayotounakos, "Exact analytic solutions of unsolvable classes of first and second order nonlinear ODEs (Part I: Abels equations)," *Appl. Math. Lett.,* **18**, 155–162 (2005).

[129] D.E. Panayotounakos and T.I. Zarmpoutis, "Construction of exact parametric or closed form solutions of some unsolvable classes of nonlinear ODEs (Abels nonlinear ODEs of the first kind and relative degenerate equations)," *Int. J. Math. and Math. Sci.,* **2011**, 387429 (2011).

[130] S.K. Turitsyn, "Spatial dispersion of nonlinearity and stability of multidimensional solitons," *Theor. Math. Phys.,* **64**, 797–801 (1985).

[131] P. Panayotaros and T.R. Marchant, "Solitary waves in nematic liquid crystals," *Physica D,* **268**, 106–117 (2014).

[132] G. Zhang and Z. Ding, "Existence of solitary waves in nonlocal nematic liquid crystals," *Nonlin. Anal.: Real World Applications,* **22**, 107-114 (2015).

[133] J.P. Borgna, P. Panayotaros, D. Rial and C. Sánchez de la Vega, "Optical solitons in nematic liquid crystals: Model with saturation effects," *Nonlinearity,* **31**, 1535–1559 (2018).

[134] D. Anderson, "Variational approach to nonlinear pulse propagation in optical fibers," *Phys. Rev. A*, **27**, 3135–3145 (1983).

[135] B. Malomed, "Variational methods in nonlinear fiber optics and related fields," *Prog. Opt.*, **43**, 71–193 (2002).

[136] G. Assanto, *Nematicons, Spatial Optical Solitons in Nematic Liquid Crystals,* John Wiley and Sons, New York (2012).

[137] W.L. Kath and N.F. Smyth, "Soliton evolution and radiation loss for the nonlinear Schrödinger equation," *Phys. Rev. E,* **51**, 1484–1492 (1995).

[138] Z. Xu, Y.V. Kartashov and L. Torner, "Upper threshold for stability of multipole-mode solitons in nonlocal nonlinear media, "*Opt. Lett.,* **30**, 3171–3173 (2005).

[139] S. Skupin, O. Bang, D. Edmundson and W. Krolikowski, "Stability of two-dimensional spatial solitons in nonlocal nonlinear media," *Phys. Rev. E,* **73**, 066603 (2006).

[140] E.I. Duque and S. Lopez-Aguayo, "Generation of solitons in media with arbitrary degree of nonlocality using an optimization procedure," *Phys. Rev. A,* **99**, 013831 (2019).

[141] S. Pu, C. Hou, K. Zhan and C. Yuan, "Dark and gray solitons in nematic liquid crystals," *Physica Scripta,* **85**, 015402 (2012).

[142] S. Pu, C. Hou, K. Zhan, C. Yuan and Y. Du, "Lagrangian approach for dark soliton in nonlocal nonlinear media," *Opt. Commun.,* **285**, 3631–3635 (2012).

[143] B.D. Skuse and N.F. Smyth, "Two-colour vector soliton interactions in nematic liquid crystals in the local response regime," *Phys. Rev. A,* **77**, 013817 (2008).

[144] B.D. Skuse and N.F. Smyth, "Interaction of two colour solitary waves in a liquid crystal in the nonlocal regime," *Phys. Rev. A,* **79**, 063806 (2009).

[145] A.A. Minzoni, N.F. Smyth and A.L. Worthy, "Modulation solutions for nematicon propagation in non-local liquid crystals," *J. Opt. Soc. Amer. B,* **24**, 1549–1556 (2007).

[146] G. Assanto, A.A. Minzoni and N.F. Smyth, "Light self-localization in nematic liquid crystals: modelling solitons in nonlocal reorientational media," *J. Nonlin. Opt. Phys. Mater.,* **18**, 657–691 (2009).

[147] N.B. Aleksić, M.S. Petrović, A.I. Strinić and M.R. Belić, "Solitons in highly nonlocal nematic liquid crystals: Variational approach," *Phys. Rev. A.,* **85**, 033826 (2012).

[148] A.V. Mamaev, A.A. Zozulya, V. K. Mezentsev, D. Z. Anderson and M. Saffman, "Bound dipole solitary solutions in anisotropic nonlocal self-focusing media," *Phys. Rev. A,* **56**, R1110–R1113 (1997).

[149] P.D. Rasmussen, O. Bang and W. Królikowski, "Theory of nonlocal soliton interaction in nematic liquid crystals," *Phys. Rev. E,* **72**, 066611 (2005).

[150] Assanto, G., García-Reimbert, C., Minzoni, A.A., Smyth, N.F., and Worthy, A.L., 2011, "Lagrange solution for three wavelength solitary wave clusters in nematic liquid crystals," *Physica D,* **240**, 1213–1219.

[151] S. Zeng, M. Chen, T. Zheng, W. Hu, Q. Guo and D. Lu, "Analytical modeling of soliton interactions in a nonlocal nonlinear medium analogous to gravitational force," *Phys. Rev. A,* **97**, 013817 (2018).

[152] K.R. Simon, *Mechanics,* Addison Wesley, 2nd Edition, Reading (MA) (1960).

[153] J.L. Synge and B.A. Griffith, *Principles of Mechanics,* McGraw-Hill, New York (1949).

[154] M. Abramowitz and I.A. Stegun, *Handbook of Mathematical Functions with Formulas, Graphs and Mathematical Tables,* Dover Publications, Inc., New York (1972).

[155] C. García Reimbert, A.A. Minzoni and N.F. Smyth, "Spatial soliton evolution in nematic liquid crystals in the nonlinear local regime," *J. Opt. Soc. Amer. B 23*, 294–301 (2006).

[156] D.J. Kaup and A.C. Newell, "Solitons as particles, oscillators, and in slowly changing media: a singular perturbation theory," *Proc. Roy. Soc. Lond. A 361,* 413–446 (1978).

[157] N.F. Smyth and B. Tope, "Beam on beam control: beyond the particle approximation," *J. Nonlin. Opt. Phys. Mater.,* **25**, 1650046 (2016).

[158] A.B. Aceves, J.V. Moloney and A.C. Newell, "Theory of light-beam propagation at nonlinear interfaces. I Equivalent-particle theory for a single interface," *Phys. Rev. A,* **39**, 1809–1827 (1989).

[159] A.B. Aceves, P. Varatharajah, A.C. Newell, E.M. Wright, G.I. Stegeman, D.R. Heatley, J.V. Moloney and H. Adachihara, "Particle aspects of collimated light channel propagation at nonlinear interfaces and in waveguides," *J. Opt. Soc. Amer. B,* **7**, 963–974 (1990).

[160] G. Assanto, N.F. Smyth and W. Xia, "Modulation analysis of nonlinear beam refraction at an interface in liquid crystals," *Phys. Rev. A,* **84**, 033818 (2011).

[161] N.F. Smyth and W. Xia, "Refraction and instability of optical vortices at an interface in a liquid crystal," *J. Phys. B: Atomic, Mol. Opt. Phys.,* **45**, 165403 (2012).

[162] G. Assanto, N.F. Smyth and W. Xia, "Refraction of nonlinear light beams in nematic liquid crystals," *J. Nonlin. Opt. Phys. Mater.,* **21**, 1250033 (2012).

[163] M. Peccianti, A. Dyadyusha, M. Kaczmarek and G. Assanto, "Tunable refraction and reflection of self-confined light beams," *Nature Phys.,* **2**, 737–742 (2006).

[164] A. Piccardi, A. Alberucci, R. Barboza, O. Buchnev, M. Kaczmarek, and G. Assanto, "In-plane steering of nematicon waveguides across an electrically adjusted interface," *Appl. Phys. Lett.,* **100**, 251107 (2012).

[165] A. Piccardi, G. Assanto, L. Lucchetti and F. Simoni, "All-optical steering of soliton waveguides in dye-doped liquid crystals," *Appl. Phys. Lett.,* **93**, 171104 (2008).

[166] F. Goos and H. Hänchen, "Ein neuer und fundamentaler Versuch zur Totalreflexion," *Ann. Phys.,* **436**, 333–346 (1947).

[167] A. Alberucci, C. P. Jisha, and G. Assanto, "Nonlinear negative refraction in reorientational soft matter," *Phys. Rev. A,* **92**, 033835 (2015).

[168] G. Assanto, A.A. Minzoni, N.F. Smyth and A.L. Worthy, 2010, "Refraction of nonlinear beams by localised refractive index changes in nematic liquid crystals," *Phys. Rev. A,* **82**, 053843 (2010).

[169] A. Alberucci, G. Assanto, A.A. Minzoni and N.F. Smyth, "Scattering of reorientational optical solitary waves at dielectric perturbations," *Phys. Rev. A,* **85**, 013804 (2012).

[170] A.I. Yakimenko, Y.A. Zaliznyak and Y.S. Kivshar, "Stable vortex solitons in nonlocal self-focusing nonlinear media," *Phys. Rev. E,* **71**, 065603(R) (2005).

[171] A. Alberucci, G. Assanto, D. Buccoliero, A. Desyatnikov, T.R. Marchant and N.F. Smyth, "Modulation analysis of boundary induced motion of nematicons," *Phys. Rev. A,* **79**, 043816 (2009).

[172] A.A. Minzoni, L.W. Sciberras, N.F. Smyth and A.L. Worthy, "Propagation of optical spatial solitary waves in bias-free nematic liquid crystal cells," *Phys. Rev. A,* **84**, 043823 (2011).

[173] A.A. Minzoni, L.W. Sciberras, N.F. Smyth and A.L. Worthy, "Nonlinear optical beams in bounded nematic liquid crystal cells," *ANZIAM J.,* **53**, pp. C373–C386 (2012).

[174] A.A. Minzoni, L.W. Sciberras, N.F. Smyth and A.L. Worthy, "Elliptical optical solitary waves in a finite nematic liquid crystal cell," *Physica D,* **301–302**, 59–73 (2015).

[175] A.A. Minzoni, L.W. Sciberras, N.F. Smyth and A.L. Worthy, "Optical vortex solitary wave in a bounded nematic-liquid-crystal cell," *Phys. Rev. A,* **87**, 013810 (2013).

[176] A. Alberucci and G. Assanto, "Propagation of optical spatial solitons in finite size media: interplay between non locality and boundary conditions," *J. Opt. Soc. Am. B,* **24**, 2314–2320 (2007).

[177] A. Alberucci, M. Peccianti and G. Assanto, "Nonlinear bouncing of nonlocal spatial solitons at the boundaries," *Opt. Lett.,* **32**, 2795–2797 (2007).

[178] A. Alberucci, A. Piccardi, U. Bortolozzo, S. Residori and G. Assanto, "Nematicon all-optical control in liquid crystal light valves," *Opt. Lett.,* **35**, 390–392 (2010).

[179] A. Piccardi, A. Alberucci, U. Bortolozzo, S. Residori and G. Assanto, "Readdressable interconnects with spatial soliton waveguides in liquid crystal light valves," *IEEE Photon. Techn. Lett.,* **22**, 694–696 (2010).

[180] G. Assanto, B.D. Skuse and N.F. Smyth, N.F., "Optical path control of spatial optical solitary waves in dye-doped nematic liquid crystals," *Photon. Lett. Poland,* **1**, 154–156 (2009).

[181] G. Assanto, B.D. Skuse and N.F. Smyth, "Solitary wave propagation and steering through light-induced refractive potentials," *Phys. Rev. A,* **81**, 063811 (2010).

[182] C. García-Reimbert, A.A. Minzoni, T.R. Marchant, N.F. Smyth and A.L. Worthy, "Dipole soliton formation in a nematic liquid crystal in the nonlocal limit," *Physica D,* **237**, 1088–1102 (2008).

[183] A.A. Minzoni, L.W. Sciberras, N.F. Smyth and G. Assanto, "Steering of optical solitary waves by coplanar low power beams in reorientational media," *J. Nonlin. Opt. Phys. Mater.,* **23**, 1450045 (2014).

[184] M. Shen, X. Chen, J. Shi, Q. Wang and W. Krolikowski, "Incoherently coupled vector dipole soliton pairs in nonlocal media," *Opt. Commun.,* **282**, 4805–4809 (2009).

[185] S. Skupin, M. Grech and W. Królikowski, "Rotating soliton solutions in nonlocal nonlinear media," *Opt. Express,* **16**, 9118–9131 (2008).

[186] X. Hutsebaut, C. Cambournac, M. Haelterman, A. Adamski and K. Neyts, "Single-component higher-order mode solitons in liquid crystals," *Opt. Commun.,* **233**, 211–217 (2004).

[187] K. T. Gahagan and G. A. Swartzlander, "Optical vortex trapping of particles," *Opt. Lett.,* **21**, 827–829 (1996).

[188] L. Yan, P. Gregg, E. Karimi, A. Rubano, L. Marrucci, R. Boyd and S. Ramachandran, "Q-plate enabled spectrally diverse orbital-angular-momentum conversion for stimulated emission depletion microscopy," *Optica,* **2** 900–903 (2015).

[189] G. Foo, D.M. Palacios and G.A. Swartzlander, "Optical vortex coronagraph," *Opt. Lett.,* **30**, 3308–3310 (2005).

[190] A. Aleksanyan and E. Brasselet, "Vortex coronagraphy from self-engineered liquid crystal spin-orbit masks," *Opt. Lett.,* **41**, 5234–5237 (2016).

[191] A. Aleksanyan and E. Brasselet, "Self-eclipsing: alignment-free vortex coronagraphy," *Opt. Lett.,* **42**, 1237–1240 (2017).

[192] A. Aleksanyan, N. Kravets and E. Brasselet, "Multiple-star system adaptive vortex coronagraphy using a liquid crystal light valve," *Phys. Rev. Lett.,* **118**, 203902 (2017).

[193] Y. Yan, G. Xie, M.J.P. Lavery, H. Huang, N. Ahmed, C. Bao, Y. Ren, Y. Cao, L. Li, Z. Zhao, A.F. Molisch, M. Tur, M.J. Padgett and A.E. Willner, "High-capacity millimetre-wave communications with orbital angular momentum multiplexing," *Nature Commun.,* **5**, 4876 (2014).

[194] N. Bozinovic, Y. Yue and Y. Ren, "Terabit-scale orbital angular momentum mode division multiplexing in fibers," *Science,* **340**, 1545–1548 (2013).

[195] R. Barboza, U. Bortolozzo, G. Assanto, E. Vidal-Henriquez, M.G. Clerc and S. Residori, "Vortex induction via anisotropy self-stabilized light-matter interaction," *Phys. Rev. Lett.,* **109**, 143901 (2012).

[196] R. Barboza, U. Bortolozzo, G. Assanto and S. Residori, "Optical vortex generation in nematic liquid crystal light valves," *Mol. Cryst. Liq. Cryst.,* **572**, 24–30 (2013).

[197] T. Sauma, R. Barboza, U. Bortolozzo, G. Assanto, M.G. Clerc and S. Residori, "Experimental characterization of the interaction law for dissipative vortex pairs," *New J. Phys.,* **15**, 013028 (2013).

[198] R. Barboza, U. Bortolozzo, G. Assanto, E. Vidal-Henriquez, M.G. Clerc and S. Residori, "Harnessing optical vortices in soft matter lattices," *Phys. Rev. Lett.,* **111**, 093902 (2013).

[199] E. Brasselet, N. Murazawa, H. Misawa and S. Juodkazis, "Optical vortices from liquid crystal droplets," *Phys. Rev. Lett.,* **103**, 103903 (2009).

[200] A.S. Desyatnikov, Y.S. Kivshar and L. Torner, "Optical vortices and vortex solitons," *Prog. Opt.,* **47**, 291–391 (2005).

[201] Y.V. Izdebskaya, A.S. Desyatnikov, G. Assanto and Y.S. Kivshar, "Dipole azimuthons and vortex charge flipping in nematic liquid crystals," *Opt. Express,* **19**, 21457–21466 (2011).

[202] Y.V. Izdebskaya, J. Rebling, A.S. Desyatnikov and Y.S. Kivshar, "Observation of vector solitons with hidden vorticity," *Opt. Lett.,* **37**, 767–769 (2012).

[203] Y.V. Izdebskaya, V.G. Shvedov, P.S. Jung and W. Krolikowki, "Stable vortex soliton in nonlocal media with orientational nonlinearity," *Opt. Lett.,* **43**, 66–69 (2018).

[204] D. Briedis, D.E. Petersen, D. Edmundson, W. Krolikowski and O. Bang, "Ring vortex solitons in nonlocal nonlinear media," *Opt. Express,* **13**, 435–443 (2005).

[205] A.A. Minzoni, N.F. Smyth, A.L. Worthy and Y.S. Kivshar, "Stabilization of vortex solitons in nonlocal nonlinear media," *Phys. Rev. A,* **76**, 063803 (2007).

[206] Z. Xu, N.F. Smyth, A.A. Minzoni and Y.S. Kivshar, "Vector vortex solitons in nematic liquid crystals," *Opt. Lett.,* **34**, 1414–1416 (2009).

[207] A.A. Minzoni, N.F. Smyth, Z. Xu and Y.S. Kivshar, "Stabilization of vortex-soliton beams in nematic liquid crystals," *Phys. Rev. A,* **79**, 063808 (2009).

[208] Y.V. Izdebskaya, W. Krolikowski, N. F. Smyth, and G. Assanto, "Vortex stabilization by means of spatial solitons in nonlocal media," *J. Opt.,* **18**, 054006 (2016).

[209] A.A. Minzoni, N.F. Smyth and Z. Xu, "Stability of an optical vortex in a circular nematic cell," *Phys. Rev. A,* **81**, 033816 (2010).

[210] Z.H. Musslimani, M. Soljačić, M. Segev and D.N. Christodoulides, "Interactions between two-dimensional composite vector solitons carrying topological charges," *Phys. Rev. E,* **63**, 066608 (2001).

[211] G. Assanto, A.A. Minzoni and N.F. Smyth, "Vortex confinement and bending with nonlocal solitons," *Opt. Lett.,* **39**, 509–512 (2014).

[212] G. Assanto, A.A. Minzoni and N.F. Smyth, "Deflection of nematicon-vortex vector solitons in liquid crystals," *Phys. Rev. A,* **89**, 013827 (2014).

[213] G. Assanto and N.F. Smyth, "Soliton aided propagation and routing of vortex beams in nonlocal media," *J. Las. Opt. Photon.,* **1**, 1000105: 105–114 (2014).

[214] M. Peccianti, A. Dyadyusha, M. Kaczmarek and G. Assanto, "Escaping solitons from a trapping potential," *Phys. Rev. Lett.,* **101**, 153902 (2008).

[215] F.A. Sala, M.M. Sala-Tefelska and M.J. Bujok, "Influence of temperature diffusion on molecular reorientation in nematic liquid crystals," *J. Nonlin. Opt. Phys. Mat.,* **27**, 1850011 (2018).

[216] U.A. Laudyn, A. Piccardi, M. Kwasny, M.A. Karpierz and G. Assanto, "Thermo-optic soliton routing in nematic liquid crystals," *Opt. Lett.,* **43**, 2296–2299 (2018).

[217] P.S. Jung, W. Krolikowski, U.A. Laudyn, M.A. Karpierz and M. Trippenbach, "Semi-analytical approach to supermode spatial solitons formation in nematic liquid crystals," *Opt. Express,* **25**, 23893 (2017).

[218] A. Ramaniuk, P. S. Jung, D. N. Christodoulides, W. Krolikowski and M. Trippenbach, "Absorption-mediated stabilization of nonlinear propagation of vortex beams in nematic liquid crystals," *Opt. Commun.,* **451**, 338–344 (2019).

[219] B.K. Esbensen, M. Bache, O. Bang and W. Krolikowski, "Anomalous interaction of nonlocal solitons in media with competing nonlinearities," *Phys. Rev. A,* **86**, 033838 (2012).

[220] U. Laudyn, A. Piccardi, M. Kwasny, B. Klus, M. A. Karpierz and G. Assanto, "Interplay of thermo-optic and reorientational responses in nematicon generation," *MDPI Materials,* **11**, 1837 (2018).

[221] E. Braun, L.P. Faucheux and A. Libchaber, "Strong self-focusing in nematic liquid crystals," *Phys. Rev. A,* **48**, 611–622 (1993).

[222] M. Warenghem, J.F. Henninot and G. Abbate, "From bulk Janossy effect to nonlinear self wave-guiding or spatial soliton in dye-doped liquid crystals," *J. Nonl. Opt. Phys. Mat.,* **8**, 341–360 (1999).

[223] M. Warenghem, J.F. Henninot and G. Abbate, "Bulk optical Freedericksz efect: non linear optics of nematics liquid crystals in capillares," *Mol. Cryst. Liq. Cryst.,* **320**, 207–230 (1998).

[224] J.F. Blach, J.F. Henninot, M. Petit, A. Daoudi and M. Warenghem, "Observation of spatial optical solitons launched in biased and bias-free polymer-stabilized nematics," *J. Opt. Soc. Am. B,* **24**, 1122–1129 (2007).

[225] J.F. Henninot, M. Debailleul, R. Asquini, A. d'Alessandro and M. Warenghem, "Self-waveguiding in an isotropic channel induced in dye doped nematic liquid crystal and a bent self-waveguide," *J. Opt. A: Pure Appl. Opt.,* **6**, 315–323 (2004).